UCRL-19075

cy 2

NOV 18 1969

LIBRARY AND
DOCUMENTS SECTION

STRUCTURE AND MECHANICAL PROPERTIES OF Fe-Ni-Mc-C STEELS

Der-Hung Huang
(M.S. Thesis)

September 1969

AEC Contract No. W-7405-eng-48

TWO-WEEK LOAN COPY

This is a Library Circulating Copy
which may be borrowed for two weeks.
For a personal retention copy, call
Tech. Info. Division, Ext. 5545

LAWRENCE RADIATION LABORATORY
UNIVERSITY of CALIFORNIA BERKELEY

UCRL-19075

cy 2

DISCLAIMER

This document was prepared as an account of work sponsored by the United States Government. While this document is believed to contain correct information, neither the United States Government nor any agency thereof, nor the Regents of the University of California, nor any of their employees, makes any warranty, express or implied, or assumes any legal responsibility for the accuracy, completeness, or usefulness of any information, apparatus, product, or process disclosed, or represents that its use would not infringe privately owned rights. Reference herein to any specific commercial product, process, or service by its trade name, trademark, manufacturer, or otherwise, does not necessarily constitute or imply its endorsement, recommendation, or favoring by the United States Government or any agency thereof, or the Regents of the University of California. The views and opinions of authors expressed herein do not necessarily state or reflect those of the United States Government or any agency thereof or the Regents of the University of California.

TABLE OF CONTENTS

ABSTRACT v
I. INTRODUCTION 1
II. EXPERIMENTAL PROCEDURE 4
A. Specimen Size and Heat Treatment 4
B. Mechanical Tests 4
C. Electron Microscopy and Fractography 5
D. Optical Microscopy 5
III. RESULTS AND DISCUSSION 6
A. Mechanical Properties 6
B. Structure of Martensite 10
C. Structure of Tempered Martensite 13
D. Structure of Bainite 16
E. Electron Fractographic Observations 19
F. Optical Microscopic Observation 21
G. Toughness of Tempered Martensite and Bainite 22
H. Fracture Path 25
I. Twinning 28
J. Precipitation of Epsilon Carbides 30
IV. SUMMARY 32
V. CONCLUSIONS 33
ACKNOWLEDGEMENTS 35
REFERENCES 36
TABLES 40
FIGURE CAPTIONS 46
FIGURES 53

STRUCTURE AND MECHANICAL PROPERTIES OF Fe-Ni-Mn-C STEELS

Der-Hung Huang

Inorganic Materials Research Division, Lawrence Radiation Laboratory,
Department of Materials Science and Engineering, College of Engineering,
University of California, Berkeley, California

ABSTRACT

The structure and mechanical properties of tempered martensite and lower bainite were investigated in a series of high purity 0.25% carbon steels with varying amounts of Ni and Mn contents. The martensites in .25C-5Ni-Fe and .25C-3Mn-Fe alloys were mainly untwinned, while those in .25C-5Ni-7Mn-Fe and .25C-7Mn-Fe alloys were heavily twinned. Also, it appeared that manganese has the effect of promoting the carbide precipitation along the lath boundaries in tempered martensite. At equivalent yield and ultimate tensile strength levels, the tempered martensite of lower manganese steels showed better impact toughness than the tempered martensite of higher manganese steels. The impact toughness (compared at similar strength levels) of untwinned tempered martensite of 0.25% carbon steel with Widmanstatten precipitation of carbide was higher than that of lower bainite, which showed unidirectional carbides.

The reasons for the difference in impact toughness between the alloys, and also between the structures were rationalized in terms of internal twinning, grain boundary precipitation and carbide morphology together with other microstructural features.

I. INTRODUCTION

In recent years, it has been argued as to whether the bainitic or martensitic structure has better toughness, when compared at the same strength level. Griffiths et al.,[1] Holloman et al.,[2] and Sachs et al.,[3] showed that the toughness of bainite obtained by isothermal transformation was lower than that of tempered martensite. Similar advantages of tempered martensite. Similar advantages of temper martensite have been reported by Banerjee,[4] Herris and Lorig,[5] and others.[6] On the other hand, opposite results have been shown by other workers.[7-14]

It seems that probably in certain cases tempered martensite may possess better toughness than bainite of similar strength levels and in some cases the reverse may be true. It has long been suspected that this controversy is due to the difference in microstructure.

It was suggested[15,16,17] that the presence of internal twinning in martensite may reduce its ductility. In a recent investigation[18] it was found that at equivalent strength levels the toughness of lower bainite was higher than that of the heavily twinned tempered martensite and suggested that the untwinned martensite possessed better toughness than that of bainite. But fully bainitic structures were not obtained in their low carbon alloys. So it remained to be seen whether the dislocated martensite (i.e. without internal twinning), was tougher than bainite or not. This is one of the aims of the present work. Furthermore, it has also been argued that the extent of internal twinning in martensite may partially depend on martensite start (M_s) temperature, the lower the M_s temperature, the greater is the tendency for martensite to twin rather than to slip.[19,20]

It is known that carbon lowers the M_s temperature drastically.

Most of the alloying elements are also known to lower the M_s temperature. Manganese has the strongest effect followed by nickel and chromium, while cobalt raises M_s. So by adjusting the composition, it is possible to vary the M_s temperature and perhaps the extent of internal twinning. Since the effect of manganese on internal twinning in martensite is not known, a series of high purity steels with varying manganese content were designed. The result of this investigation will add to the existing empirical results of the effect of carbon and nickel in increasing the extent of internal twinning in martensite.

Also, manganese is an important component of practically all steels and is, therefore, of fundamental interest. Manganese content is a significant factor in determining the degree of brittleness exhibited by steel. It is added to steel because it reacts with excess sulfur to prevent hot-shortness (high temperature brittleness). Manganese also acts as a deoxidizing agent to overcome oxygen-induced intergranular brittleness.[21] It is also responsible for the solid-solution strengthening of ferrite.[22] All the investigators agree that manganese lowers transition temperature, but no universal agreement has been reached regarding the mechanism by which this is achieved. It has been reported that manganese additions improved the toughness of the steel.[23-26] But it is interesting to note the structure of all these commercial steels consists of ferrite and pearlite and none of them contain more than 2% of manganese. The famous Hadfield's manganese steel (~10-14% Mn) is fairly tough and is austenitic. There are a few investigations concerning the effect of manganese on martensitic steels. It has been reported by Decker et al.[27] that the toughness of 18% Ni maraging steel is lower by increasing manganese from 0.07 to 0.23%. The ratio of notch

tensile strength to tensile strength drops from 1.32 to 0.62 when manganese content is changed from 0.07 to 1.9%. In an effort to partially substitute manganese for nickel in 18% Ni maraging steel, Patterson et al.[28] found that manganese was deleterious to toughness when it exceeded 2.25%. They tentatively attributed this to some kind of interaction of manganese with other alloying elements, e.g. titanium and cobalt. The effect of manganese on the toughness of Fe-C martensitic steels without any titanium or cobalt is not understood. So, by using a series of high purity 0.25% carbon alloys with varying manganese contents, an attempt has been made in the present work to investigate whether manganese is injurious to the toughness of tempered martensitic steels or not, and if so, why?

The compositions of the alloys under investigation are given in Table I along with their M_s temperatures. The steels will be referred to by their heat numbers as given in Table I.

II. EXPERIMENTAL PROCEDURE

A. Specimen Size and Heat Treatment

Tensile specimens whose dimensions are shown in Fig. 1(a) were 0.060 inch thick. Standard full size Charpy V-notch specimens, Fig. 1(b), were used for measuring the impact toughness. All the specimens were cut parallel to the rolling direction. The specimens were austenitized at 1650°F for one and half hour in an argon atmosphere and then either water (for low manganese steel) or oil quenched (for high manganese steel). Then they were immediately immersed in liquid nitrogen and refrigerated for 20 hours to ensure complete transformation to martensite. Tempering was done in a neutral salt bath. All the specimens were double tempered for 4 hours at different temperatures, i.e. tempered for 2 hours, water quenched, then refrigerated, and finally tempered for another 2 hours. This completely eliminated the retained austenite. Bainite was obtained by quenching the specimens directly into the salt bath and isothermal transforming at the required temperature. Fully bainitic structures were checked as will be discussed in a later section. Carbon analysis before and after heat treatment showed no significant decarburization. Nevertheless, after heat treatment, tensile specimens were carefully ground with removal of 0.010 inch from both sides in order to eliminate any possible effects of surface decarburization from austenitizing. Flood cooling was employed to minimize specimen heating during grinding.

B. Mechanical Tests

Tensile tests were performed on an Instron machine at a cross head speed of 4×10^{-2} in/min. A Sonntag Universal testing machine with a capacity of 240 ft-lbs was used to impact the Charpy V-notch specimens. All tests were conducted at room temperature, i.e. 77°F.

C. Electron Microscopy and Fractography

Thin foils for transmission electron microscopy were prepared by light mechanical grinding from 0.060 inch thick heat treated specimens to about 0.040 inch. Then chemically polished to about 0.005 inch in a 50% solution of phosphoric acid and hydrogen-perioxide. They were electropolished by the window technique first in perchloric-acetic acid (1:10) solution which gave a rapid thinning. Final electropolishing was accomplished in the well-known chromic-acetic acid (75 grams CrO_3, 400 ml acetic acid and 21 ml H_2O) at 25 dc volts and 20°C. Foils were examined in a Siemens Elmiskop IA microscope, operated at 100 KV.

The replicas for electron microscope examination of the freshly broken fracture surface of Charpy specimens were prepared by a two-stage plastic/carbon technique.[29] The contrast was increased by shadowing with either platinum-palladium (80:20) or chromium at an angle of 45 degrees. The carbon replicas were examined in the electron microscope at 60 KV.

D. Optical Microscopy

Thin sections were cut from the broken Charpy impact specimens and conventional metallographic polishing techniques were used. Observation and photography were done with a Carl Zeiss Optical Microscope.

III. RESULTS AND DISCUSSION

A. Mechanical Properties

The mechanical properties of tempered martensite and bainite are tabulated in Tables II and III, respectively. The results are the average of two to four tests, with very litte scatter in the data. The purpose of tempering at various temperatures is to obtain different strength levels, thus the toughness can be compared on the basis of equivalent yield strength or ultimate tensile strength, which is very important.

Figures 2 through 7 show the variation of mechanical properties versus tempering temperature. Steels with 5% nickel, i.e. 804, 805 and 806 (Figs. 2, 3, and 4) show similar tempering characteristics. The yield and ultimate tensile strengths drop and elongation and Charpy V-notch impact energy increases with tempering temperature, as expected. By comparing steel 804 (0% Mn), 805 (2% Mn), and 806 (4% Mn), it can be seen that the addition of first 2% Mn is very effective in increasing in tempering resistance. The Charpy V-notch toughness of 805 and 806 show an embrittlement when tempered around 600°F. This is so-called 500°F embrittlement of tempered martensite, which generally occurs through the range of 400 ~ 700°F. It is interesting that this does not exist in steel 804 and the degree of embrittlement increases from steel 804 to steel 805, to steel 806, in that order. This increase in degree of 500°F embrittlement of tempered martensite with increasing manganese content is very similar to that observed by Payson[30] in carbon steels, where increasing carbon also enhances 500°F embrittlement. 500°F embrittlement has been associated with the resolution of epsilon carbide and simultaneous replacement be cementite.[31] But in the present case,

as will be discussed later, it is observed that the carbide is mainly cementite with a small amount of epsilon carbide when the tempering temperature is 400°F. This indicates that epsilon carbide has started to dissolve at the temperature lower than 400°F. While at 600°F, the carbides are predominantly cementite. So the embrittlement should have occurred somewhere closer to 400°F instead of at 600°F if the argument is valid. It is rather difficult to attribute the embrittlement to the resolution of carbides.

Figures 5, 6 and 7 show the tempering behavior of steel 807, 808 and 809, respectively. Again the yield and ultimate tensile strength drop and elongation generally increases with tempering temperature. Similar to steel 806, steels 807 and 808 show embrittlement when the tempering temperature is 600°F. Steel 807 possesses high toughness when the strength is low. However the CVN impact energy for steel 808 and 809 are so low, that the toughness never exceeds 20 ft-lbs through the whole range of strength levels. The mechanical properties will be correlated with structure later.

In order to show the variation of toughness with manganese content at similar strength levels curves are drawn in Fig. 8(a) and (b) for steel 804, 805 and 806. All the points are interpolated from Fig. 2 to Fig. 7 and listed in Table IV. It can be seen that the toughness of 5Ni-.25C steel increases slightly up to addition of 2% manganese but drops at higher manganese contents. Figures 9(a) and (b) show the same relation of toughness with manganese content at different yield and ultimate strength levels for steels 807, 808 and 809. Here, it is clear that the toughness of 0.25% carbon martensitic steel drops with increasing manganese from 3 to 7 percent. Thus it is concluded that the manganese

addition in excess of 2 ~ 3% is deleterious to the toughness of plain Fe-Ni-0.25 carbon tempered martensitic steel.

The Charpy V-notched toughness obtained at various yield and ultimate tensile strength for different heats are also shown in Fig. 10 and Fig. 11. As usual, steels 804, 805 and 807 show that toughness decreases with increasing strength, while the steels with higher manganese, i.e. 806, 808 and 809 are very brittle and the toughness values are low even at low strength levels. At equivalent strength level the marked difference in toughness between lower and higher manganese steel indicates that increased manganese content above 3% tends to lower the toughness of tempered martensite which is undesirable.

The mechanical test data of the bainitic steels are given in Table III. The mechanical properties of as-transformed bainite are relatively poorer than that of tempered martensite of the same steel. The yield strength drops and the toughness increases with increasing isothermal transformation temperature. To compare the toughness of martensite with bainite, it is very important to ensure that a fully bainitic structure is obtained, because alloys of mixed structure of martensite and bainite possess very low toughness. The presence of almost 100% bainite in steels 804, 805 and 807 was verified by examining the microstructure of bainite after tempering at low temperatures. In this case the carbide morphology in bainite and in tempered martensite would be different and so the presence of any martensite in as-transformed bainite could be detected. Usually mechanical properties of a fully bainitic structure do not change much by tempering, a slight lowering of strength may be observed. On the other hand, a mixed structure of bainite and martensite will show somewhat different mechanical properties after tempering. The

toughness data of any incompletely transformed bainite, i.e. mixture of bainite and martensite, should not be used in comparing the toughness of bainite with tempered martensite. The results in Table III further exclude the possibilities of any mixed structure in steels 804, 805 and 807. In steel 808 it was rather difficult to obtain a fully bainitic structure. Furthermore, not a single bainite plate or lath was observed in steels 806 and 809 when isothermally transformed at 510°F for 24 hours.

The comparison of toughness between lower bainite and tempered martensite is shown in Fig. 12 by plotting CVN impact value against strength for the two structures. All the data have been given in Table II and IV and summarized in Table V to facilitate the comparison. Only the results of steel 804, 805 and 807 are used, because fully bainitic structure of higher manganese steel, i.e. 806, 808 and 809 were not obtained. It can be seen that at similar strength level, the toughness of bainite of steel 804, 805 and 807 are much inferior compared to that of tempered martensite. The strength levels of bainite are limited due to the restriction on the isothermal transformation temperature, i.e. higher isothermal transformation temperature gives upper bainite which is not desired.

Summarizing the above results we can say that at similar yield and ultimate strength levels, the tempered martensitic structure of steel of lower manganese (i.e. 804, 805 and 807) shows better toughness compared to that of the steels of high manganese (i.e. 806, 808 and 809). In other words, the toughness of martensitic steel decreases with increasing manganese content. As will be seen later, the structural observations show that the steels 806, 808 and 809 contain relatively more internal twinning compared to steels 804, 805 and 807. The tempered martensite of

steels 804, 805 and 807 has better toughness than the bainite of the same steel.

B. Structure of Martensite

In manganese steels, epsilon martensite forms at relatively high manganese contents. In the presence of carbon and nickel, the minimum amount of manganese required to form epsilon martensite is not known. Thus, it was necessary to ascertain the martensite phase of the present alloys. It was found that the alloys under investigation, formed alpha martensite instead of epsilon phase. This was verified in two ways. Firstly, all the selected area diffraction patterns of electron microscopy of martensite were identified to be body centered structure corresponding to alpha martensite. Secondly, by using x-ray metallographic technique, no epsilon martensite or retain austenite but only alpha martensite was detected in steel 804 through 809. However, in steel 953 with M_s temperature of 148°F about 5 ~ 10% of retained austenite was detected after quenching and storing in liquid nitrogen for 372 hours.

The microstructure of martensite in dilute alloys of Fe-Ni system has been described as massive martensite by Owen et al.,[32] self-accommodating martensite by Christian,[33] needle-like or lath martensite by Kelly and Nutting.[34] The high carbon martensite structure was characterized by Lucas[35] as an "acicular crystal-like substance." To avoid the confusion in terminology, martensite will be described by its substructure, i.e. twinned martensite or dislocated (untwinned) martensite.

The structure of martensite of steel 804 is shown in Fig. 13. Dense dislocations can be seen inside the narrow laths similar to the observation of Kelly and Nutting.[34] This steel is almost completely free of internal twinning and is typical of dislocation martensite. The lath size

varies from area to area but always fallsinto the range of 0.25μ in Fig. 13(a) to 1μ in Fig. 13(b), which is another area of the structure. The structure of martensite of steel 805 is shown in Fig. 14, which is also mainly untwinned. Several families of martensite laths with no twinning at all is shown in Fig. 14(a). Sometimes, very fine microtwins are observed in some narrow martensite laths as in Fig. 14(b). The existence of microtwins have been reported recently[36,37] and will be discussed later. Another region, Fig. 14(c), shows the martensite laths nucleated and grew from the prior austenite grain boundary. Dislocation network can also be seen in the martensite plate at the right hand region of the micrograph. A fair amount of twinning was observed in the martensite of steel 806 as shown in Fig. 15. Many examples of completely internally twinned martensite are seen in steel 953 as observed in Fig. 16(a). Analysis of selected area diffraction pattern indicates that the orientation of the matrix are twin are [110] and [$\bar{1}\bar{1}0$] respectively. The twin plane is ($\bar{1}12$). In addition to the twin spots there are other spots due to double diffraction [Fig. 16(c)]. Dark field of (002) twin spots reverses the contrast of the twins.

The morphology of martensite in steel 807 is similar to that of 804 and is shown in Fig. 17. Figure 17(a) shows a group of narrow dislocated martensite laths with no twinning at all. Various sizes of martensite laths of two families also seen in Fig. 17(b). The structure shows that martensite of steel 807 is practically untwinned. Martensite of steel 808 is found to consist of mainly laths with small amount of plates. Some internal twinning in martensite of steel 808 is observed. Figures 18(a) and (b) show the internal twinning in martensite plate and lath respectively. It seems that the twins in the plate are comparatively bigger than those

in the laths. Martensite of steel 809 is found to consist of a fair amount of internal twinning. Figure 19(a) shows a twinned plate in the same steel. Sometimes the twins are restricted to only a few martensite plates and also to the midrib of the grain [Fig. 19(b)]. This kind of morphology has also been observed before. Figure 19(c) shows a heavily twinned region of martensite of the same steel.

Quantitative measurements of the amount of lath and the volume fraction of twins in martensite are rather difficult. However, by examining a number of foils, a relative comparison could be made. It is found that the amount of lath martensite in steel 804 is more than that in steel 953. And it is also noticed that the amount of internal twinning in martensite increases gradually from steel 804 to 805, to 806 and 953 in that order. The only difference in composition among these alloys is in their manganese content. Steel 804 contains 0%; 805, 2%; 806, 4% and 953, 7% of manganese. It is clear from the foregoing observation that manganese promotes internal twinning in martensite. Also, results of the observation of steels 807 and 809 reveal that the martensite in 0.25%C - 3% Mn (steel 807) is practically untwinned, while that in 0.25%C - 7%Mn (steel 809) is moderately twinned. This further confirms that the extent of internal twinning increases with increasing Mn content. It is concluded that manganese has the effect of promoting internal twinning in martensite. This is contradictory to what is stated by Christian.[33] He indicated that the martensite in high-alloy steels containing manganese is not internally twinned.

Since manganese has the effect of decreasing M_s temperature, and it is observed that internal twinning in martensite increases with manganese content, then the extent of internal twinning in martensite depends

partially on M_s temperature is true in pure Fe-Ni-Mn-C and Fe-Mn-C alloys as it is Fe-C[34] and Fe-Ni-C[19] but not in Cobalt bearing alloys.[18]

C. Structure of Tempered Martensite

The microstructures of martensite at various temperatures have also been examined. The martensite of steel 804 tempered at 400°F showed a mixture of epsilon carbide and cementite. In many cases these precipitates do not give a sufficiently satisfactory diffraction pattern to be identified, but the trace analysis of the habit plane shows a {100} habit. It is known that the epsilon carbide has $\{100\}_\alpha$ habit and grows in $\langle 100\rangle_\alpha$ direction. Also some cementite with {110} habit has also begun to form as can be seen from Fig. 20(a) and (b) where the arrows indicate the cementite. In some other areas, the resolution of epsilon carbide and the precipitation of cementite seems complete as observed in Fig. 20(c) where the foil orientation is ⟨111⟩ and all the three families of {110} cementite upon increasing the tempering temperature. Figure 21 shows the structure of martensite of steel 804 tempered at 600°F. At this tempering temperature the precipitates are all found to be cementite with {110} habit, which agrees with the observation by others.[38-40] Spherodized carbides of 200Å to 500Å diameter are found on tempering at 850°F [Fig. 22(a) and (b)]. The structures begin to recover at this temperature. Figure 22(c) and (d) show the structure of martensite of the same steel tempered at 1000°F for 2+2 hours. The carbides agglomerate on the martensite lath boundary in oblate spheroid shape. Polygon networks in recovered grains are clearly revealed, but some needle-like grains still persist as shown in Fig. 22(c). When tempered at 1050°F for 80 hours, big spherodized carbides and individual dislocations are obtained in the recrystallized ferrite grains as seen in Fig. 23(a) and (b).

The tempering resistance of steel 804 which contains no manganese is relatively poor in comparison with the steels containing manganese. This is revealed by comparing steel 804 with steel 807 both from microstructure and strength variation with temperature.

It is also known that in the presence of twins the cementite precipitates preferentially on the twin boundaries with {112} habit.[41] Figure 24 shows the structure of martensite of steel 805 tempered at 400°F, which shows a packet of internally twinned martensite laths with carbides, precipitated on the twin-matrix interface. The selected area diffraction pattern shows the matrix to be in approximately $[\bar{1}\bar{3}1]$ and the twins to be approximately $[10\bar{1}]$. Twinning on $(\bar{1}21)$ plane will bring $[\bar{1}\bar{3}1]$ matrix into an orientation which is about 5 to 6 degrees off from $[10\bar{1}]$. This is similar to the observation of Kelly and Nutting on high carbon steels.[34] Dark field of $(0\bar{2}0)$ twin spot reverses the contrast of the twins. Carbides are also revealed by dark field, of spot A as shown in Fig. 24(c), and it can be seen that these carbides precipitate on the twin boundaries. Figure 24(d) is the dark field of $(\bar{1}0\bar{1})$ matrix spot which coincides with $(10\bar{1})$ twin spot and the whole group of laths have lighted up. Not only the boundary of the packet but also the lath boundary can be seen clearly. This proves that these are laths instead of plate. The observation of microtwins in the lath is further confirmed. This indicates that the inhomogeneous shear in massive or lath martensite does not have to be slip. Thus, the morphology of martensite, i.e. plate or lath does not depend on substructure, i.e. whether twin is present or not. Therefore, it would be more appropriate to classify martensite by their substructures, i.e. twinned or untwinned instead of by the morphology.

Figure 25 shows the structure of martensite of 805 tempered at 800°F where cementite precipitates uniformly in Widmanstatten pattern. This

structure will be used to compare with the bainitic structure to explain the discrepancy in toughness between the two structures. Figure 26(a), (c) and (d) show 600°F, 850°F and 1000°F tempered martensite in steel 807. All of them show Widmanstatten precipitation of cementite, the Fe_3C becoming coarser at higher temperature. By comparing 22(a) with 26(c) it is seen that when tempered at 850°F the carbide in steel 804 has begun to spherodize while that of steel 807 has not. The morphological difference between the carbides of steel 804 and 807 is even more clear at 1000°F. As can be seen in Fig. 22(d) and Fig. 26(d), spherodized carbides of 1000 ~ 2000Å diameter are found in 1000°F tempered martensite of 804 while the carbides still more or less maintain their platelet shape in martensite of 807 at 1000°F. It is evident that steel 807 possesses stronger tempering resistance than steel 804. This agrees with the variation of strength with temperature as shown in Fig. 2 and Fig. 5. The compositions of steel 804 and 807 are .025C-5Ni-Fe and .25C-3Mn-Fe respectively. Thus, as an alloying element in steel, manganese gives a stronger tempering resistance than nickel.

Unlike the lower manganese steels (i.e. steels 804, 805 and 807), tempering of higher manganese steels (806, 808 and 809) shows a fair amount of long precipitates along the lath boundaries and the carbide distribution is rather non-uniform. Also, as described before, manganese promotes internal twinning, which provides a preferential site for cementite to precipitate. Thus the tempered high manganese steels seem to contain long precipitates along both twin and lath boundaries. Figure 27 (a) shows continuous carbide precipitates all along the lath boundary obtained after tempering steel 809 at 400°F. Dark field reveals a part of the carbides [Fig. 27(b)]. Aside from the continuous precipitates at

the twin boundaries, Widmanstatten precipitation in the twin free regions is also observed as shown in Fig. 27(c) which is another area of the foil. 400°F tempered martensite of steel 808 is also observed, long twins and carbides precipitates can be seen in Fig. 28. On tempering at 600°F, again, martensite of steel 806 shows long and continuous carbide precipitates all along the twin boundaries, as can be seen in Fig. 29(a), together with some Widmanstatten carbides. Dark field of a twin spot reversed the contrast of the twins [Fig. 29(b)]. But tempering the same steel at 400°F did not show a pronounced lath boundary precipitation. Figure 30 shows the structure 800°F tempered martensite of steel 809, where long, coarse carbide precipitates are observed. On tempering at 1000°F, carbides in the matrix became coarser. Also, long precipitate along the boundaries broke up into segments to minimize the total free energy. The structure of 100°F tempered martensite of steel 808 is shown in Fig. 31. Figure 32 indicates that the precipitates along the twins of martensite of steel 806 have also fragmented into sections upon tempering at 1000°F for 2+2 hours.

Summarizing the above results, we can say that in lower manganese steels, epsilon carbide precipitates below 400°F, and is subsequently replaced by cementite at higher tempering temperatures. The manganese containing steel has stronger tempering resistance than a nickel steel. In higher manganese steels, the cementite precipitates preferentially along the twin and lath boundaries suggesting that manganese may promote lath boundary precipitation.

D. Structure of Bainite

It has long been known that there are two different bainite morphologies, namely upper and lower bainite.[42] In many steels a distinct micro-

structral difference between these two forms has been seen. In upper bainite the carbides frequently form elongated particles between the bainitic ferrite grains, while in lower bainite, the carbides tend to precipitate at an inclined angle of 55 ~ 65° to the major growth direction, or longitudinal axis, of the bainitic ferrite grain.[42,43] Since the mechanical properties of upper bainite are relatively poor, only isothermally transformed lower bainite is of interest in this study. The conventional transition temperature from lower to upper bainite is known to be around 650°F. According to Pickering,[44] the maximum temperature above which no lower bainite forms depends on the carbon content of the alloy. His results show that it is about 900°F for 0.25% carbon steel. The highest transformation temperature adopted in this work is 760°F and it will be seen that the structures are all lower bainites.

Figure 33(a), (b) show the structure of lower bainite of steel 804 transformed at 720°F and 760°F for 24 hours respectively. The bainite lath are found to be placed side by side with only a small misorientation between them as checked by selected area diffraction pattern. This agrees with the nucleation model proposed by Hehemann[45] and Pickering.[44] The bainite laths are very similar to low carbon martensite laths except that there are carbides inside the ferrite laths. The carbides are identified to be cementite and the trace analysis indicates that these habit plane of the carbides is {112} similar to the observation made by Baker et al.[40] No internal twinning was observed in bainitic ferrite, the reason why the cementite precipitated on only {112} planes still needs further investigation. Steel 804 was also transformed at 720°F for 60 hours. The structure does not show any significant difference from that of transformed for 24 hours at the same temperature, i.e. 720°F. This

indicates that as soon as the transformation is complete, prolonging the time does not affect the structure significantly. It is found that generally the strength decreases and the toughness increases with increasing transformation temperature. The structure of bainite of steel 807 transformed at 710°F and 760°F are shown in Fig. 34 (a) and (b). They show that carbide particles become coarser and probably the structure recovered to a greater extent at higher transformation temperature. Thus the reason for decrease in strength and increase in toughness with increasing transformation temperature for lower bainite may be a direct strength-toughness relationship.

At lower transformation temperatures, wider bainite laths or plates are observed instead of narrow laths. This is seen in Fig. 35 which is the lower bainite of steel 805 isothermally transformed at 610°F for 24 hours, where the bainite lath is wider than those transformed at 720°F and 760°F as shown in Fig. 33 and 34.

As mentioned before the bainitic reaction in steel 808 did not go to completion. Figure 36 is the structure of steel 808 after isothermal transformation at 610°F for 24 hours, followed by tempering at 610°F for 2+2 hours. It shows a mixed structure of bainite and martensite. Typical undirectional bainitic carbides making an angle of 55 ~ 652 to the longitudinal axis of the ferrite lath are seen in the upper right hand portion. While in the center and left portion, both twin and Widmanstatten carbides (not clear shown in the print) indicates the martensite formed from untransformed austenite on cooling after isothermal transformation. For steels 806 and 809, no bainite was obtained even after transforming for 24 hours. In contrast, full bainite was obtained in steels 804, 805 and 807. It is evident that in the presence of high manganese content, the bainitic transformation becomes rath sluggish. For a further investi-

gation of the effect of manganese on bainite, it is necessary to determine its effect on the TTT diagrams.

E. Electron Fractographic Observations

The fracture surface of Charpy V-notch specimens tested at room temperature were replicated by two stage plastic/carbon replica technique and examined for the fracture mode.

The tempered martensite of lower manganese steels possess relative high toughness and show dimple rupture. Figure 37(a) (b) and (c) represent the fracture surfaces of martensite of steel 804 tempered for 2+2 hours at 400°F, 850°F and 1000°F respectively. They show equiaxed dimples in Fig. 37(a) and elongated dimples in (b) and (c) which are typical ductile failure. Dimples are believed to occur by the formation, growth and coalescence of microvoids. Such voids are often initiated by hard dispersed particles in steel.[46,47]

The fracture surfaces of tempered martensite and bainite of similar strength levels were also examined. Figure 38(a) represents the fracture mode in martensite of steel 805, tempered at 800°F. The main feature in it is that the fracture surface is composed largely of well-defined dimples of various sizes. In contrast, the fracture mode in bainite of the same steel transformed at 610°F, shows a mixture of dimples and cleavage facets, which is a low energy fracture [Fig. 38(b) and (c)]. This agrees with the toughness data which gave CVN values of 48 and 13.5 ft-lbs for the tempered martensitic and bainitic structures respectively. The mixed structure of cleavage facets and dimples in bainite indicates that when a cleavage crack is arrested, some deformation and ductile fracture occur until a new crack is initiated. Fracture mode comparison of the tempered martensite with bainite of similar strength level was also

made for steel 807. Figure 39(a) shows the fracture surface of 800°F tempered martensite of steel 807 where small equiaxed dimples are observed. The fracture surface of bainite of the same steel transformed at 710°F [Fig. 39(b)] indicates the herringbone structure, which is typical of cleavage.[48] There are at some boundaries dark irregular bands where the carbon replicating film has collapsed, suggesting very large level difference or intergranular cracks at these boundaries as observed by Low.[49] The CVN toughness values of these tempered martensite and bainite are 43 and 26 ft-lbs respectively.

From the above comparison, it is clear that the fracture mode agrees with the impact data which further confirms that tempered martensite of these alloys is tougher than bainite. Fractographs of the martensite of steel 806 and 808 and 809 tempered at various temperatures are also presented in Fig. 40. Almost all of them show predominantly intergranular fracture. Some small dimples were occasionally seen. The observations also match the low impact toughness values of these higher manganese steels. Figure 40(a) shows the fracture mode of 400°F tempered martensite of steel 806, which contains flat dimples together with groups of small dimples. While for the same material tempering at 600°F shows a fracture mode which is almost completely intergranular, as observed in Fig. 40(b). Since this is a very low energy fracture, it implies that the boundaries of the twins or laths are weaker at 600°F than that at 400°F; this agrees with the observation that lath boundary precipitation is more prominent at 600°F than at 400°F. The fracture surface of martensite of steel 808, tempered at 600°F and 1000°F are shown in Fig. 40(c) and (d) respectively. Though both show intergranular failure but the former has a lower impact toughness than the latter. This agrees with the observation that

at higher tempering temperature, the continuous carbide breaks up into segments and the structure is more or less recovered. The same argument applies to the martensite of steel 809 when tempered at 400°F and 1000°F respectively, [Fig. 40(c) and (f)].

Summarizing the above description we can say that the fracture mode of tempered martensite of lower manganese steel is dimple-rupture, that of bainite is a mixture of cleavage and dimple-fracture, that of tempered martensite of higher manganese steel is predominantly intergranular failure. It will be discussed later what kind of grain boundary does the fracture path follow in higher manganese steel.

F. Optical Microscopic Observation

It has been reported that the brittleness in quenched and tempered steels are due to the presence of microcracks.[7] Marder and Krauss[48] also observed microcracks in quenched martensite specimens that were above 0.67 percent carbon. Martensite of higher manganese content which showed low toughness were metallographically prepared and examined. Figure 41(a) and (b) are the structures martensite of steels 806 and 808 respectively. No microcracks in any of the high manganese steels were observed. Thus the low impact toughness of tempered martensite of high manganese steel could not be due to the presence of microcracks.

Figure 42 is the optical micrograph of steel 953 obtained after quenching from austenizing temperature and storing in liquid nitrogen for 372 hours, which shows a mixed structure of martensite with 5 to 10 percent of retained austenite.

G. Toughness of Tempered Martensite and Bainite

Based on similar strength levels, toughness was compared either between tempered martensite of varying manganese content or between different structures of the same composition such as tempered martensite and bainite.

1. Comparison of Toughness Between Bainite and Tempered Martensite of Lower Manganese Steels with a Little Twinning.

The test results show that tempered martensite of lower manganese steel possesses better toughness than bainite. Assuming other things being equal, the difference in toughness will be attributed to the grain size and orientation of ferrite, and carbide morphology.

Both the size and orientation of the grains are important in controlling the toughness. It is known[49] that the smaller the grain size the greater is the energy absorbed during fracture and the more difficult is the process of crack propagation. In the present case, various sizes of laths were found in both bainite and martensite, but generally it seems that the bainite laths are narrower than the martensite laths. However, the contribution to toughness by narrow laths of bainite is superseded by other factors, as discussed below.

As mentioned before, the fracture mode of the bainite of the steels under investigation is predominantly cleavage. It has been shown from structure observations that the bainite consists mainly of laths, which are separated from each other by low angle boundaries. It is thought that the cleavage cracks can propagate easily in these laths. If the bainite consisted of randomly oriented grains the change in orientation at individual grain boundaries impeded the propagation of the cleavage crack by causing localized deformation near the boundary and would absorb

more energy. However in the structure of parallel laths, less energy seems to be required for the crack to propagate. The reason for this is that low angle boundaries between the neighboring ferrite laths in bainite do not have a strong blocking effect in diverting the direction of the cracks which can subsequently retard the crack propagation. Thus, the cleavage crack can cross from one ferrite grain to another without much deviation in direction until the crack meets the prior austenite grain boundaries. This can be one of the factors responsible for the low toughness of bainite.

Also, the morphology of the carbide precipitation affects the toughness. In the twin free region of martensite, carbides precipitate in Widmanstatten pattern, while in the bainitic structure, relatively few, coarse, widely spaced carbides precipitate unidirectionally inside the ferrite grain. It can be seen that the chance of the crack being blocked by Widmanstatten precipitates of carbide is greater than that of the bainitic carbides. Thus, so far as the resistance to crack propagation is concerned, the morphology of carbides in tempered martensite is better that of the bainitic carbides. This may be another main factor which is responsible for the difference in toughness between the two structures.

The above argument can be demonstrated by comparing Fig. 34(a) with Fig. 26(c). These show the structure of bainite and tempered martensite of steel 807 at equivalent yield strength level of about 130 ksi. The bainitic structure [Fig. 34(a)]shows not only high dislocation density but also a few unidirection carbides, while the tempered martensitic structures [Fig. 26(c)] of the same strength level as bainite shows numerous uniformly distributed caribdes on {110} planes. Similar comparison can also be made for bainite (Fig. 35) and tempered martensite (Fig. 25) for steel 805.

2. Comparison of Toughness Between Tempered Martensite of High and Low Manganese Steels

The mechanical tests results have shown that the toughness of martensite of lower manganese steel is higher than that of higher manganese steel. Again assuming other things being equal, the difference in toughness may partially be attributed to microstructural difference such as internal twinning and partially to grain boundary precipitation.

The role of internal twinning in lowering the toughness can be explained as follows. As seen before, in the presence of twins the cementite precipitates preferentially all along the twin boundaries. Thus the carbides are very long and continuous as shown in Figs. 27-32. These long precipitates of carbides allow a twin boundary to act as a strong barrier for the movement of dislocations. Thus dislocations pile up in the localized areas and induced high stress concentration, which nucleates a crack and accelerates the propagation. Evidence of cracks induced by twins in metals and alloys have been observed before.[49,51] Also, in the presence of internal twinning, the martensite is more likely to be deformed by mechanical twinning rather than slip as reported by Krauss et al.[52] It is known that the plastic deformation is restricted when the deformation mode is mechanical twinning which subsequently results in low toughness. Therefore, the presence of internal twinning and its effect on the carbide precipitation in the martensite plate together with deformation by mechanical twinning can give rise to the low energy fracture.

The presence of precipitation or segregation at the grain boundary is another major reason for lowering the toughness and causing intergranular failure. Sometimes, these grain boundary precipitates need

not be continuous to produce intergranular fracture as reported by other workers.[53,54] Grain boundary precipitates help in nucleation of cracks by acting as a strong barrier to dislocation motion and to the transfer of plastic energy from grain to grain. The grain boundary carbides were very prominant in the martensite of higher manganese steels. Long carbides were detected both along grain boundaries and twin boundaries. These long carbides are thought to be responsible for the low toughness. The fracture path giving rise to the intergranular failure will be treated in another section.

H. Fracture Path

1. The Fracture Path of Tempered Martensite in High Manganese Steel

The fracture modes of higher manganese steel, e.g., 806, 808 and 809 are predominantly intergranular. A statistical measurement of the apparent grain size as obtained from all the fractographs show that the average grain size is even smaller than ASTM No. 12 while in 0.25% carbon steel, generally austenite grain sizes are in the range of ASTM No. 7-8,[55] when the austenitizing temperature is about 1700°F. This indicates that the intergranular failure of the present alloys does not follow the prior austenite grain boundaries. Furthermore, the electron microscope observations show the carbides to precipitate either along the lath boundary or twin boundary. Continuous precipitation along the prior austenite grain boundary was not detected. So the lath or twin boundaries but probably not the prior austenite grain boundaries are weakened by the carbide precipitates. Therefore, the fracture path follows the weakest portion of the ferrite. Also it is well known that in 0.2% carbon steel, the martensite which is made up of "packets of parallel plates or laths" form within a prior austenite grain, as schematically shown in Fig. 43,[56] which is for three packets of martensite. Section A represents a packet

of martensite. Blocks of different orientations are found within a packet as represented in Section B. The slip structure is evident within each block as seen in Section C which corresponds to the laths seen in the electron microscope.

The grain size as seen in the fractographs are probably the same size as these martensite packets, and so it is likely that the fracture path might follow the boundary between the packets. It appears that manganese promotes carbide precipitation along the ferrite lath boundaries in the tempered martensite and subsequently causes embrittlement.

2. The Fracture Path in Bainite of Lower Manganese Steels

The fracture mode of bainite is predominantly cleavage, together with some small dimples as shown in Fig. 38(b), (c) and Fig. 39(b). As mentioned before, the carbides precipitate unidirectionally on {112} planes inside the ferrite laths of lower bainite. In the absence of lath boundary precipitation, the {112} planes in the matrix may be the weak planes and the crack is most probably nucleated at the carbide-matrix interface, i.e., {112} planes. Moreover, the herringbone pattern [Fig. 39(b)] further suggests that the failure is along {112}.[48] Therefore the cleavage of bainite of low manganese steel follows {112} planes.

Since the fracture appearance of bainite of steel 807 isothermally transformed at 710°F for 24 hours shows a herringbone structure, which has been associated with the cleavage along {112} twin-matrix interface in martensite,[48] one may think this is an indication of the existance of transformation twins in bainite. However, no apparent internal twinning has been detected in lower bainitic structure in the present work which agrees with the observations of other workers.[44,45] Also, no

positive evidence of the presence of internal twins in lower bainite has ever been reported. Since Tekin and Kelly[41] have suggested that during tempering the twins are removed from martensite by the precipitation of cementite. Analogous to this, Shackleton and Kelly[43] postulated that the bainitic ferrite that forms martensically from austenite may also be twinned and these twins can also be removed by the precipitation of cementite during isothermal transformation. This not only elucidates the reason why the habit planes and orientation relationships of the cementite in lower bainite are consistant with the carbide precipitation on twins in tempered martensite but also explains the causes which is responsible for the failure of detecting internal twinning in lower bainite. In spite of this it is rather difficult to understand why should the internal twins, if there is any, in bainite be removed at 710°F while that the microtwins in martensite persist even tempered at 1000°F which is higher than the transformation temperature for bainite. In fact, based on their theoretical investigation on the crystallography of bainite transformation, Bowles et al.[57] have reported that twinning can not explain the crystallographic features of low bainite such as habit plane and the austenite-ferrite orientation relationship. Since there is no conclusive direct evidence of the presence of internal twinning in lower bainite, whether the bainite is twinned or not needs further investigation.

Thus, although the herringbone structure of the fracture surface of bainite suggests the cleavage along {112} matrix-twin interface, this can also be {112} matrix-carbide interface as explained in the beginning of this section. Besides, even if the herringbone structure in the present case is a resultant of cleavage along twin-matrix interface, the type of the twins should be mechanical twins which arises during deformation,

instead of transformation twins. Because the width of the bainitic ferrite lath in steel 807 [Fig. 34(a)] is about 0.25 to 0.5μ which is very much small in compare with the appearance of the "twins" shown in the fractograpy [Fig. 39(b)]. No matter how, whether it is twin-matrix interface or matrix-carbide interface, the argument that the cleavage follows {112} planes in lower bainite of low manganese steel seems still valid.

I. Twinning

The martensite of steel can be described by its transformation substructure i.e. twinned martensite and dislocated martensite. The factors which basically affect the twinning in martensite have been a subject of discussion over the past decade. The M_s temperature has been generally agreed to be one of the main parameters in affecting twinning by most researchers.[17-20]

It is observed in the present work that the martensites of .25C-3Mn-Fe and .25C-5Ni-Fe alloys are mainly untwinned, but the martensite of .25C-7Mn-Fe and .25C-5Ni-7Mn-Fe alloys are almost fully twinned. Since manganese is known to lower the M_s temperature and it has been shown that the internal twinning in martensite is promoted by manganese. Thus the extent of internal twinning in martensite depends partially on M_s temperature is further confirmed in pure Fe-Ni-Mn-C and Fe-Mn-C alloys as it is in Fe-C[34] and Fe-Ni-C[19] but not in cobalt bearing alloys.[18]

Fundamentally, the deformation mode of bcc materials, i.e. whether they deform by twinning or slip depends on the critical resolved shear stress (CRSS) for slip or twinning at the transformation temperature. At the transformation temperature if the CRSS for twinning is lower than that for slip then the structure should be twinned. On the other

hand, the structure should be deformed by slip if the CRSS for slip is lower than that for twinning. It is known that CRSS for slip in body centered materials is strongly temperature dependent. Thus at low temperatures, the CRSS for slip may be so high that twinning is the only mode of deformation. Generally the lower the transformation temperature, the greater is the tendency for martensite to twin. It is clear that the deformation mode (i.e. twin or slip) is temperature dependent. Also, martensite start (M_s) to martensite finish (M_f) covers a range of about 200°C.[58] So in many cases mixed structures of slipped and twinned martensites are observed. The required stress is supplied by the stress induced from transformation. It is known that CRSS is composition dependent. Therefore, not only the M_s temperature, but also the effect of composition on CRSS is important in determining whether the martensite will twin or slip. From the present work it appears that manganese not only decreases M_s temperature but may also reduce CRSS for twinning. A further understanding about the structure of martensite can be reached as soon as the relation of CRSS with individual alloying elements is established.

In addition to the lowering of transformation temperatures, Kelly and Nutting[17] indicated that by raising the stacking fault energy of the austenite should also favor twinning in martensite. The correlation of stacking fault energy in twinning seems to be true in adding carbon and nickel into steel. Because both elements promote twinning in martensite, lower M_s temperature and raise the stacking fault energy of austenite. But manganese is known to decrease the stacking fault energy of austenite. According to Kelly and Nutting, this should not favor twinning. However this is not the case, thus the indication that the stacking fault energy of austenite affects twinning in martensite does not seem to be true.

Some work on chromium steel has also been done. A 0.18C-4Cr-Fe[59] alloy shows an mainly untwinned structure. In 18-8 stainless steel,[60] the alpha martensite transformed from stress induced epsilon martensite does not show internal twinning. Similarly, martensite in Fe-8Cr-1.1C ($M_s \approx -34°C$)[61] steel shows only a little twinning. The lowering of M_s temperature by chromium is similar to that by manganese, but the effect of chromium on twinning is not known and is currently under investigation. It has been shown here that the addition of manganese up to 7% enhances internal twinning in body centered (α) martensite. In manganese steels, epsilon martensite forms at relatively high manganese contents. The effect of the manganese on twinning in alpha martensite when it coexists with the epsilon phase has not yet been studied.

J. Precipitation of Epsilon Carbides

There is a small amount of evidence as to the presence of epsilon carbide in tempered low carbon martensite (< .25%C). The first stage of tempering of martensite has been generally assumed to be a discontinuous process resulting in a metastable equilibrium of epsilon carbide and low carbon martensite(.25%C).[62] From this it was concluded that a steel having 0.25% carbon or less should be undersaturated with respect to epsilon carbide and thus should not form epsilon carbide precipitates upon tempering. However, the presence of epsilon carbide in tempered steels containing less than 0.25% carbon have been detected by x-ray diffraction technique.[63] In a recent investigation, Barton[64] reported that in a low carbon, high nickel, internally twinned, plate martensite, (-11C-28Ni-Fe), epsilon carbide precipitated on tempering at low temperatures. Based on the observation that epsilon carbide forms in low carbon twinned martensite he suggested that the tempering characteristics of

a martensite may be more directly related to the martensite morphology than to the carbon content of martensite. However, it is known that both the morphology and the substructure of martensite are affected by the carbon content. It is difficult to understand whether or not there is any direct effect of the martensite morphology or substructure on the precipitation of epsilon carbide. The morphology of carbide depends on the substructure of martensite, but the type of carbide formed does not seem to be affected by the martensite morphology and structure directly. The present observation of epsilon carbide in practically untwinned lath of steel 804 when tempered at 400°F is an evidence that the epsilon carbide can also precipitate in untwinned martensite lath upon tempering at lower temperatures. Thus the correlation, if there is any, between the morphology of martensite with the precipitation of epsilon carbide should be examined more closely.

Actually, when a supersaturated solid solution decomposes to form new phases, the transformation tends to follow the lowest energy path, where not only volume free energy but also surface energy and strain energy factors should be taken into consideration. Epsilon carbide generally precipitates earlier than cementite upon tempering. It is expected that epsilon carbide is either thermodynamically or kinetically favorable in the first stage of tempering. No systematic investigation of this aspect has been done. However, it has been reported[65] that the movement of iron atoms in ferrite to form epsilon carbide appear to be less complicated that the required for cementite. This might be one of the kinetic factor which favors the formation of epsilon carbide.

IV. SUMMARY

By means of microstructural and fractographic investigation, it has been shown that the fracture mode of practically untwinned tempered martensite of low manganese steels is a typical dimple rupture which is associated with high energy failure. The fracture modes in lower bainite of low carbon steels exhibit cleavage facets mixed with some small flat dimples, while the fracture appearance of twinned tempered martensite of higher manganese steels is predominantly intergranular which is typical of low energy failure.

Microstructural examination shows that the high impact toughness of untwinned tempered martensite is associated mainly with uniform Widmanstatten {110} precipitation of carbide and the absence of both internal twins and lath boundary precipitates. Even in the absence of internal twinning and lath boundary precipitation, the bainite shows lower toughness. Because the bainitic carbides precipitate unidirectionally on {112} planes, which not only weaken the {112} planes to cause cleavage but also exert less resistance to the crack propagation. In contrast to the untwinned martensite of low manganese steel, the martensite of higher manganese content shows a mixed morphology of twinned plates and laths. Upon tempering continuous carbides precipitate preferentially along the twin and lath boundaries, which subsequently cuases intergranular fracture along the lath boundaries.

The low energy fracture mode of tempered martensite of high manganese steel seems to result from the effect of the presence of internal twins coupled with the enhanced lath boundary precipitation.

V. CONCLUSIONS

1. The structure of martensite in a 0.25% carbon steel with higher manganese content (7% Mn) exhibits greater amounts of internal twinning than the low manganese ($\leq$ 3% Mn) ones. Thus manganese promotes internal twinning in the martensite.

2. At similar yield and ultimate tensile strength levels, the tempered martensite of low manganese steels (which is mainly untwinned) shows better toughness than the tempered martensite of higher manganese steel (which is twinned).

3. It appears tha manganese promotes carbide precipitation along the lath boundaries of tempered martensite. This coupled with the effect of manganese on twinning may be responsible for the low toughness of high manganese steels.

4. At equivalent strength levels, the toughness of untwinned tempered martensite of 0.25% carbon steel with Widmanstatten precipitation of carbides is higher than that of lower bainite, which shows unidirectional carbides.

5. The fracture mode of high manganese ($\geq$ 4%) tempered martensitic steel shows predominantly intergranular failure. The fracture does not seem to occur entirely along the prior austenite grain boundaries, but mostly along the ferrite lath boundaries.

6. In the lower bainite, the strength decreases and toughness increases with increasing isothermal transformation temperature. This follows the usual strength-toughness relationship.

7. No apparent transformation twins are observed in lower bainitic ferrite. At lower transformation temperature, wider bainitic laths or plates are observed. Relatively narrower laths are observed at higher

transformation temperatures.

8. The carbides precipitate on {112} planes in the ferrite matrix of lower bainite. The cleavage plane of lower bainite may be {112}.

9. Isothermal transformation of steel to bainite becomes sluggish in the presence of high manganese ($\geq$ 4%). This is due to the effect of manganese on the kinetics of transformation.

10. The 500°F embrittlement of tempered martensite is enhanced by increasing the manganese content.

11. The addition of manganese to carbon steel offers a greater tempering resistance than the equal amount of nickel does.

12. In pure Fe-Mn-C and Fe-Ni-Mn-C alloys the M_s temperature is an indication of the extent of internal twinning in body centered martensite.

ACKNOWLEDGEMENTS

The author is deeply grateful to Professor Gareth Thomas for his personal guidance, encouragement and support throughout the course of this work. He is also thankful to the Republic Steel Corporation for supplying the alloys and the to the staff of its research center for helpful discussions. Special thanks are due to Mr. Santosh Das for valuable discussions and help during the course of the work. The excellent technical assistance of Pat Shand and Jane Ball is also very much appreciated.

This work was done under the auspices of the United States Atomic Energy Commission through the Inorganic Materials Research Division of the Lawrence Radiation Laboratory.

REFERENCES

1. W. T. Griffiths, L. B. Pfeil, N. P. Allen, JISI, 12 (1939) 343.

2. J. H. Holloman, L. D. Jaffe, D. E. McCarthy, and M. R. Norton, Trans. ASM 38 (1947) 807.

3. G. Sachs, L. J. Ebert, and W. F. Brown, Trans. AIME 176 (1948) 424.

4. B. R. Banerjee, ASTM Special Technical Publications 370 (1967) 30.

5. S. A. Herres and C. H. Lorig, Trans. ASM 40 (1948) 775.

6. Report on Physical Properties Influenced by As-Quenched Hardness. Society of Automotive Engineers, Iron and Steel Technical Committee, Report No. MR-73, 1947.

7. E. S. Davenport, E. L. Roff, E. C. Bain, Trans. ASM 10 (1939) 228.

8. E. E. Legge, Metals and Alloys, 10 (1939) 228.

9. E. S. Davenport, Trans. ASM 27 (1939) 837.

10. L. J. Klinger, W. J. Barnett, R. P. Frohmberg and A. R. Troiano, Trans. ASM 46 (1954) 1557.

11. R. F. Hehemann, V. J. Luhan and A. R. Troiano, Trans. ASM 49 (1957) 409.

12. B. J. Waterhouse: Discussion, "Physical Properties of Martensite and Bainite," Special Report 93, The Iron and Steel Institute (London), p. 147 (1965).

13. J. S. Pascover and S. J. Matas, ASTM Special Publication No. 370 (1965).

14. K. J. Irvine and F. B. Pickering, JISI, 201 (1963) 518.

15. G. Thomas, D. Schmatz and W. Gerberich, High Strength Materials, V. F. Zackay, ed., (John Wiley and Sons, Inc., New York, N. Y. (1965), p. 324.

16. O. Johari and G. Thomas, Trans. ASM 58 (1965) 563.

17. P. M. Kelly and J. Nutting, JISI 197 (1961) 199.

18. S. Das and G. Thomas, Trans. ASM, September 1969 (in press).

19. R. L. Patterson and C. M. Wayman, Acta Met. 12 (1964) 1306.

20. O. Johari and G. Thomas, Acta Met. 13 (1965) 1211.

21. W. P. Ress and B. E. Hopkins, JISI, 172 (1952) 403.

22. C. E. Lacy and M. Gensamer, Trans. ASM 32 (1944) 88.

23. W. Barr and A. J. K. Honeyman, JISI, 157 (1947) 239.

24. J. Gorrissen, JISI, 162 (1949) 16.

25. F. W. Boulger and R. H. Frazier, Trans. AIME, 200 (1954) 645.

26. J. Heslop and N. J. Petch, Phil. Mag. 2 (1957) 649.

27. R. F. Decker, J. T. Eash and A. J. Goldman, Trans. ASM 55 (1962) 58.

28. W. R. Patterson and L. S. Richardson, Trans. ASM, 59 (1966) 71.

29. A. Phillips, V. Kerlins and B. V. Whiteson, Electron Fractography Handbook, Technical Report ML-TDR-64-416 (January 31, 1965).

30. P. Payson, Trans. AIME, November (1954) 1242.

31. B. R. Banerjee, JISI, 203 (1965) 166.

32. W. S. Owen, E. A. Wilson and T. Bell, in High Strength Materials, V. F. Zackay, ed., (John Wiley and Sons, Inc., New York, N. Y., 1965), p. 167.

33. J. W. Christian, Iron and Steel Institute, Special Report No. 93, p. 1 (1963).

34. P. M. Kelly and J. Nutting, Proc. Royal Soc. A259 (1960) 45.

35. F. F. Lucas, American Soc. Steel Treating 6 (1924) 669.

36. R. W. Messler, Jr., G. S. Ansell, and V. I. Lizvnov, Trans. ASM, 62 (1969) 362.

37. S. Das and G. Thomas, Trans. AIME (in press).

38. W. C. Leslie, Acta Met. 9 (1961) 1004.

39. W. Pitch, Acta Met. 10 (1962) 897.

40. A. J. Baker, P. M. Kelly and J. Nutting, in Electron Microscopy and Strength of Crystals, G. Thomas and J. Washburn, eds., (Interscience Publishers, New York, N. Y., 1963), p. 899.

41. E. Tekin and P. M. Kelly, Precipitation from Iron-Base Alloys, AIME (1963).

42. Electron Microstructure of Bainite in Steel. Second Progress Report by Subcommittee XI of Committee E-4, ASTM Proc. 52 (1952) 543.

43. D. N. Shackleton and P. M. Kelly, The Iron and Steel Institute, Special Report No. 93 (1965) 126.

44. F. B. Pickering in Symposium: Transformation and Hardenability in Steels, Climax Molybdenum Co., (1967), p. 45.

45. J. M. Oblak and R. F. Hehemann in Symposium: Transformation and Hardenability in Steels, Climax Molybdenum Co., (1967), p. 109.

46. C. D. Beachem, An Electron Fractographic Study of Mechanism of Ductile Rupture in Metals, U.S. Naval Research Laboratory, NRL Report 5871 (1962).

47. C. D. Beachem and R. M. N. Pelloux, Electron Fractography - A Tool for the Study of Micro-Mechanics of Fracturing Processes, Symposium on Fracture Toughness Testing and Its Application, ASTM (1964).

48. C. D. Beachem, The Crystallographic of Herringbone Fracture in an Iron-Chromium-Aluminum Alloy, U.S. Naval Research Laboratory, Report of NRL Progress, January 1967, p. 28.

49. J. R. Low, Jr., in Fracture, B. L. Averbach, et al., eds., (M.I.T. Press, Cambridge, Mass., 1959), p. 68.

50. A. R. Marder and G. Krauss, Trans. ASM 60 (1967) 651.

51. A. Gilbert, et al., Acta Met. 12 (1964) 754.

52. G. Krauss and W. Pitsch, Acta Met. 12 (1964) 278.

53. J. Plateau, G. Henry and C. Crussard, Rev. universelle mines 12 (1956) 1.

54. J. Plateau, G. Henry and C. Crussard, Rev. met., 54 (1957) 3.

55. I-T Diagrams, 1963, published by United States Steel Corporation.

56. J. M. Marder and A. R. Marder, Trans. ASM 62 (1969) 1.

57. J. S. Bowles and N. F. Kennon, J. Aust. Inst. Met. 5 (1960) 106.

58. K. W. Andrews, JISI, July (1965) 721.

59. E. W. Page, P. Manganon, Jr., G. Thomas, and V. F. Zackay, Trans. ASM 62 (1969) 45.

60. P. Manganon, Strengthening and Phase Transformations in 304 Stainless Steel, Ph.D. Thesis, University of California, Berkeley, 1968.

61. K. Shimizu and C. M. Wayman, Acta Met. 14 (1966) 1390.

62. C. Roberts, B. Averbach and M. Cohen, Trans. ASM 45 (1953) 576.

63. C. Altstetter, Trans. AIME 224 (1962) 394.

64. C. J. Barton, Acta Met. 17 (1969) 1085.

65. K. W. Andrews, Acta Met. 11 (1963) 939.

TABLE I

Chemical Composition of the Alloys (Given in wt. %)

With Their Ms Temperature

Heat No.	C	Ni	Mn	P	S	Ms Temp. °F
804	.26	5.0	---	.004	<.005	603
805	.26	4.9	1.9	.004	<.005	520
806	.26	4.85	3.8	.005	<.005	385
807	.25	---	3.0	.004	<.005	601
808	.25	---	4.9	.007	<.005	454
809	.24	---	6.85	.005	<.005	367
953*	.26	5.1	7.5	ND	ND	148

* Steel 953 contains 0.02% Si and 0.02% Al.

ND: Not Determined

Table II.

Mechanical Properties of Tempered Martensitic Structures*

Heat No.	Tempering Temperature of	ys $\times 10^3$ psi (0.2% offset)	uTs $\times 10^3$ psi	% Elongation	Hardness R_c	CVN Impact Energy Ft-lb
804	400	173.4	200.7	9.24	43.5	23
	600	150.2	167.3	9.5	37	35
	750	124	135.6	10.71	30.5	54
	800	114.4	124.5	10.73	27	64
	850	103	114	11.02	23	73
	900	96.2	107	12.9	21	87
	1000	81.2	94.1	16.6	17	118.2
805	400	171.5	202	8.32	44.5	21.5
	600	168.7	185.7	8.53	42	18
	800	134.2	144.5	10.48	33.5	48
	1000	107.2	122.5	14.9	26	78.25
806	400	171.9	207.5	10.7	45	27
	600	171.7	192.2	9.32	41	5.75
	800	158.2	167.2	11.66	38	14
	1000	119.5	134.7	14.6	31	18.5
807	400	175.3	206.3	7.82	44.5	16.5
	600	174	188.2	8.4	40.5	13.5
	800	139	153.3	11.6	34	43.25
	850	131	142.7	12.75	32	52.5
	1000	107.3	119.8	14.3	25	95.25
808	400	176	211	8.57	46	9.5
	600	171.8	185.5	8.44	44	4.88
	800	158.2	167.7	9.28	39	17.75
	1000	117.6	130.4	12.3	29	15.5

Table II., continued

Heat No.	Tempering Temperature of	ys $\times 10^3$psi (0.2% offset)	uTs $\times 10^3$psi	% Elongation	Hardness R_c	CVN Impact Energy Ft-lb
809	400	172.7	209.5	10.14	46	4
	600	169.1	200	10.17	44	4.75
	800	162.3	182.3	11.66	42	7.75
	1000	126.9	141.2	13	32	8.5

* Double Tempered at each temperature for 2 + 2 hours.

Table III.

Mechanical Properties of Bainitic Structures*

Heat No.	Isothermal Transformation Temperature °F	Tempering† Temperature °F	YS $\times 10^3$psi (0.2% offset)	UTS $\times 10^3$psi	Elongation %	Hardness R_c	CVN Impact Energy ft-lb
804	720		93.7	105.7	11.9	21.5	81
	720	600	92.5	105	11.5	21	-
	760		82	98.3	13.7	36	89
	760	590	81.5	96.9	12.1	36	-
805	610		136	155.7	10.44	33	13.5
	610	600	135	153.5	9.32	33	-
	660		123.65	142.85	11.71	32	10
	660	600	121.7	137.7	8.59	33	-
807	710		133.7	147.2	12.9	33	26
	710	600	130.4	143.2	11.51	32	-
	760		112.2	124.7	11.3	26	43.5
	760	590	111.2	124.3	12.4	24	-
808	610		138.1	182.3	9.32	39	-
	610	610	145.4	172.5	8.82	38.5	-

* Isothermal transformation time is 24 hours

† Double tempered at each temperature for 2 + 2 hours

TABLE IV

Interpolated Toughness Values (Ft - lb) at Various Yield

or Ultimate Strength of Tempered Martensite

Heat No.	Interpolated Toughness Values (Ft - lb) at Various Strength Levels									
	Yield Strength (Ksi)						Ultimate Tensile Strength (Ksi)			
	120	130	140	150	160	170	140	160	180	200
804	58	---	42	---	30.5	---	50	38	30	---
805	63	---	41	---	24	---	54	35	22	---
806	19	---	18	---	13	---	18	16	10	---
807	---	54	---	28	---	16	---	32	18	15
808	---	18	---	18	---	6	---	18	8	6
809	---	8	---	8	---	6	---	8	8	6

TABLE V

Comparative Toughness Values of Tempered Martensitic and Bainitic Structure at Similar Strength Levels

Heat No.	Strength Levels, Ksi	CVN Impact Energy, Ft - lb.	
		Tempered Martensite	Bainite
804	Y.S ~ 94	92	81
	UTS ~ 106	90	81
804	Y.S ~ 82	118	89
	UTS ~ 98	108	89
805	Y.S ~ 136	45	13.5
	UTS ~ 156	38	13.5
805	Y.S ~ 124	59	10
	UTS ~ 143	50	10
807	Y.S ~ 134	47	26
	UTS ~ 147	46	26
807	Y.S ~ 112	85	43.5
	UTS ~ 125	83	43.5

FIGURE CAPTIONS

Fig. 1 The dimensions of mechanical test specimens.

Fig. 2 The effect of tempering temperature of the strength and toughness of steel 804.

Fig. 3 The effect of tempering temperature of the strength and toughness of steel 805.

Fig. 4 The effect of tempering temperature of the strength and toughness of steel 806.

Fig. 5 The effect of tempering temperature of the strength and toughness of steel 807.

Fig. 6 The effect of tempering temperature of the strength and toughness of steel 808.

Fig. 7 The effect of tempering temperature of the strength and toughness of steel 809.

Fig. 8 Variation of Charpy V-notch impact energy with manganese content for steel 804, 805 and 806 at (a) similar yield strength, (b) similar ultimate tensile strength.

Fig. 9 Variation of Charpy V-notch with manganese content for steel 807, 808 and 809 at (a) similar yield strength, (b) similar ultimate tensile strength.

Fig. 10 Comparison of Charpy V-notch impact energy of various steel at different yield strength levels.

Fig. 11 Comparison of Charpy V-notch impact energy of various steel at different ultimate strength levels.

Fig. 12 Comparison of CVN toughness between tempered martensite and bainite.

Fig. 13 Transmission electron micrograph of martensite of steel 804. (a) typical dislocated martensite lath which is in the absence of internal twinning, (b) another region shows wider laths. The width of the laths varies from 0.25μ to 1μ.

Fig. 14 Structure of martensite in steel 805. (a) shows untwinned martensite lath of several families. (b) another region showing some fine internal twins in some of the narrow laths. (c) another region shows the martensite laths nucleated and growing from the prior austenite grain boundary. Dislocation network can also be seen in the martensite plate (right hand side).

Fig. 15 Martensite of steel 806 shows a twinned structure.

Fig. 16 (a) bright field micrograph of martensite in steel 953 showing heavily twinned structure, (b) dark field of (002) twin spot reverses the contrast of the twins, (c) selected area diffraction pattern with analyzed pattern showing the orientation of the matrix and twin curve [110] and [$\bar{1}\bar{1}0$], respectively, extra spots are due to double diffractions. The twinning phase is ($\bar{1}12$).

Fig. 17 Structure of martensite of steel 807 showing no internal twinning. (a) group of parallel, narrow, dislocated martensite laths of 0.5μ in width, (b) another area showing two families of martensite lath.

Fig. 18 Martensite of steel 808. (a) showing uneven distributed twins in a martensite plate, (b) showing microtwins in the martensite lath.

Fig. 19 Structure of martensite of steel 809 showing (a) slightly thicker twins in the martensite plate, (b) twinning in the mid-rib of the martensite plate, (c) another region with heavily twinned structure.

Fig. 20 Martensite of steel 804 double tempered at 400°F for 2 + 2 hours. (a) showing fine precipitates of epsilon carbide, arrow marks indicates cementite of {110} habit has also begun to precipitate, (b) shows another region with epsilon carbide and cementite, as in (a), (c) another region with higher magnification, showing cementite only, all three families of {110} cementite are in contrast, foil orientation ⟨111⟩.

Fig. 21 (a) Structure of martensite of steel 804 after tempered at 600°F for 2 + 2 hours showing Widmanstatten pattern of cementite, (b) dark field image reverses the contrast of the cementite.

Fig. 22 Martensite of steel 804, (a) and (b) double tempered at 850°F for 2 + 2 hours, show spherodized carbides of 200 ~ 500 Å diameter in the matrix which has started to recover; (c) and (d) double tempered at 1000°F for 2 + 2 hours, show polygon networks in recovered structure, some needle-like grain still persists, carbides agglomerate on the martensite lath boundaries.

Fig. 23 Martensite of steel 804 tempered at 1050°F for 80 hours shows a recrystallized structure. (a) big spherodized carbides with individual dislocations, grain boundary fringes are observed in the upper left hand corner, (b) another region showing carbide precipitates in recrystallized ferrite grain.

Fig. 24 Structure of martensite of steel 805 tempered at 400°F for 2 + 2 hours. (a) shows a packet of internally twinned martensite laths with carbides precipitated on the twin-matrix interface, (b) dark field of $(0\bar{2}0)$ twin spot reverses the contrast of the twins, (c) dark field of carbide spot A lights up the twins, it is clear that cementite precipitateson the twin boundaries, (d) dark field of $(\bar{1}0\bar{1})$ matrix spot lights up the whole packet of martensite laths, (e) selected area diffraction pattern and indexed diffraction pattern showing the orientation of the matrix and twin are approximately $[\bar{1}3\bar{1}]$ and $[10\bar{1}]$, respectively. Twin plane is $(\bar{1}21)$.

Fig. 25 Martensite of steel 805 tempered at 800°F for 2 + 2 hours, Widmanstatten pattern of cementite precipitates uniformly inside the matrix.

Fig. 26 Martensite of steel 807 tempered at 2 + 2 hours at: (a) 600°F, shows fine Fe_3C precipitates with $\{\bar{1}10\}$ habit, (b) dark field lights up the carbides, (c) 850°F, Fe_3C becomes coarser, (d) 1000°F, cementite still remains in its platelet or rod-like shape, but part of them has begun to spherodize.

Fig. 27 (a) bright field of 400°F tempered martensite of steel 809 shows continuous carbide precipitations all along the lath boundaries, (b) dark field shows part of the carbides, (c) another area shows cementite precipitates on the twins also in the matrix.

Fig. 28 Martensite of steel 808 tempered at 400°F for 2 + 2 hours. (a) shows fair amount of twins and carbide precipitates in the matrix, (b) dark field of a twin spot reverses the contrast of the twin.

Fig. 29 (a) Martensite of steel 806 tempered at 600°F for 2 + 2 hours, long and continuous cementite precipitates along the twins boundaries, some Widmanstatten Fe_3C are also in faint contrast, (b) dark field of a twin spot reveals the twins.

Fig. 30 Structure of martensite of steel 809 tempered at 800°F for 2 + 2 hours, long, coarse cementite precipitate on twins.

Fig. 31 1000°F double tempered martensite of steel 808 showing the continuous Fe_3C along the lath boundaries has become coarser and broken into segments to minimize the total energy.

Fig. 32 Martensite of steel 806 tempered at 1000°F for 2 + 2 hours showing the cementite precipitates along the twin boundaries have also fragmented into sections.

Fig. 33 Lower bainite of steel 804 obtained by isothermally transforming at (a) 720°F and (b) 760°F for 24 hours. Both show side by side nucleated ferrite laths. The carbides precipitate at an angle of 55 ~ 65° to the long direction of the ferrite lath. The width of the lath is about 0.25 to 0.5 μ, (b) shows a structure recovered to a greater extent than (a).

Fig. 34 Structure of lower bainite after isothermal transformation for 24 hours at (a) 710°F, shows relatively few carbides, (b) 760°F, carbides become coarser.

Fig. 35 Lower bainite in steel 805 formed at 610°F after transforming for 24 hours, showing wider bainitic ferrite lath of plate than high temperature transformed bainite as shown in Figs. 33 and 34. Notice the carbides are relatively few, widely-spaced and coarser as compared to Fig. 25 which is the tempered martensite of the same steel with similar strength level.

Fig. 36 Structure of steel 808 isothermally transformed at 610°F for 24 hours, followed by tempering at 610°F for 2 + 2 hours shows a mixed structure of bainite with tempered martensite. Typical unidirectional bainitic carbides making an angle of 55 ~ 65° to the longitudinal axis of the ferrite lath are seen in the upper right hand corner of the micrograph. Martensite twins together with Widmanstatten Fe_3C (not clearly shown in the print) are also seen in the center and left regions.

Fig. 37 Electron fractograph of martensite of steel 804 tempered for 2 + 2 hours at (a) 400°F, showing equiaxed dimples, 23 ft-lbs, (b) 850°F, showing elongated dimples, 73 ft-lbs, (c) 1000°F, showing elongated, high energy dimples, 18 ft-lbs. All are typical of ductile failure.

Fig. 38 Electron fractograph of tempered martensite and bainite of similar strength level of steel 805. (a) 800°F, tempered martensite showing various sizes of well-defined dimples, 48 ft-lbs, (b) and (c) show the fracture mode of bainite obtained by isothermally transformed at 610°F for 24 hours, mixture of dimples and cleavage fracture. Cleavage steps are seen in the right region of (b), 13.5 ft-lbs.

Fig. 39 Electron fractograph of tempered martensite and bainite of similar strength level of steel 807. (a) 800°F tempered martensite, showing equiaxed dimples, 43 ft-lbs, (b) lower bainite formed at 710°F after transforming for 24 hours, showing herringbone structure, which is typical of cleavage along {112} crystallographic planes. Dark irregular bands are the collapsed carbon films, indicating a large level difference along the boundary. 26 ft-lbs.

Fig. 40 Electron fractograph of (a) 400°F tempered martensite of steel 806 shows small dimples together with big flat dimples, 27 ft-lbs., (b) 600°F tempered martensite of 806 shows predominantly integranular failure, 5.75 ft-lbs., (c) 600°F tempered martensite of 808, 5 ft-lbs., (d) 1000°F tempered 808, 15.5 ft-lbs., (e) 400°F tempered martensite of 809, 4 ft-lbs., (f) 1000°F tempered martensite of 809, 8-5 ft-lbs., (b) to (f) all show predominantly intergranular failure.

Fig. 41 Optical micrograph of (a) as quenched martensite of steel 806, (b) martensite of steel 808 tempered at 1000°F for 2 + 2 hours, no microcrack is detected. All etched with 2% nital.

Fig. 42 Optical micrograph of steel 953 obtained after quenching from austenitizing temperature and storing in liquid nitrogen for 372 hours which shows a mixed structure of martensite with 5 to 10 percent of retained austenite. Etched with 2% nital.

Fig. 43 Schematic drawing of three packets of lath martensite within a prior austenite grain. Section A represents a packet. Section B shows blocks within a packet and Section C illustrates an aligned substructure within the block of a packet.[56]

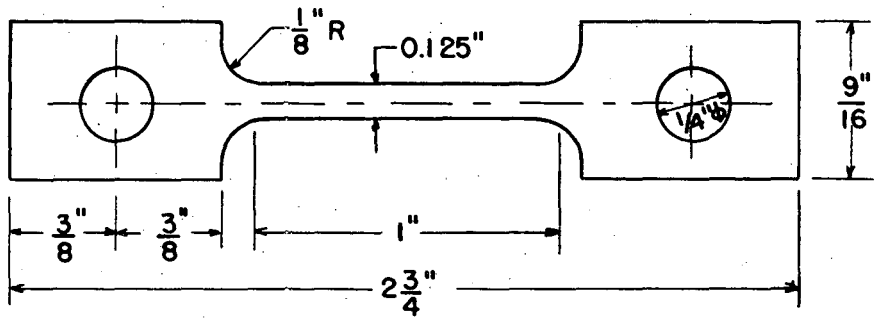

(a) TENSILE SPECIMEN THICKNESS = 0.06"

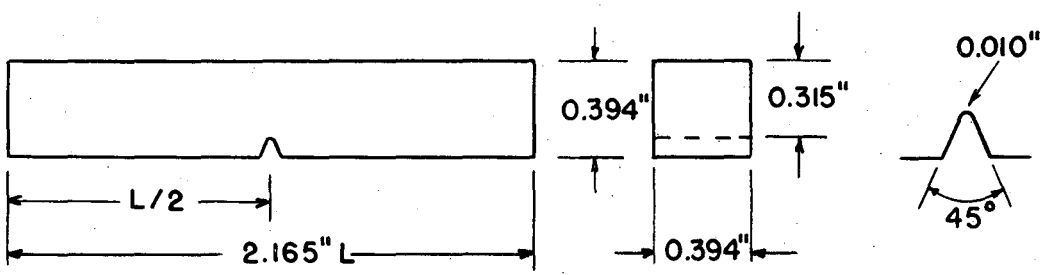

(b) CHARPY V-NOTCH IMPACT SPECIMEN.

XBL 698-1314

Fig. 1

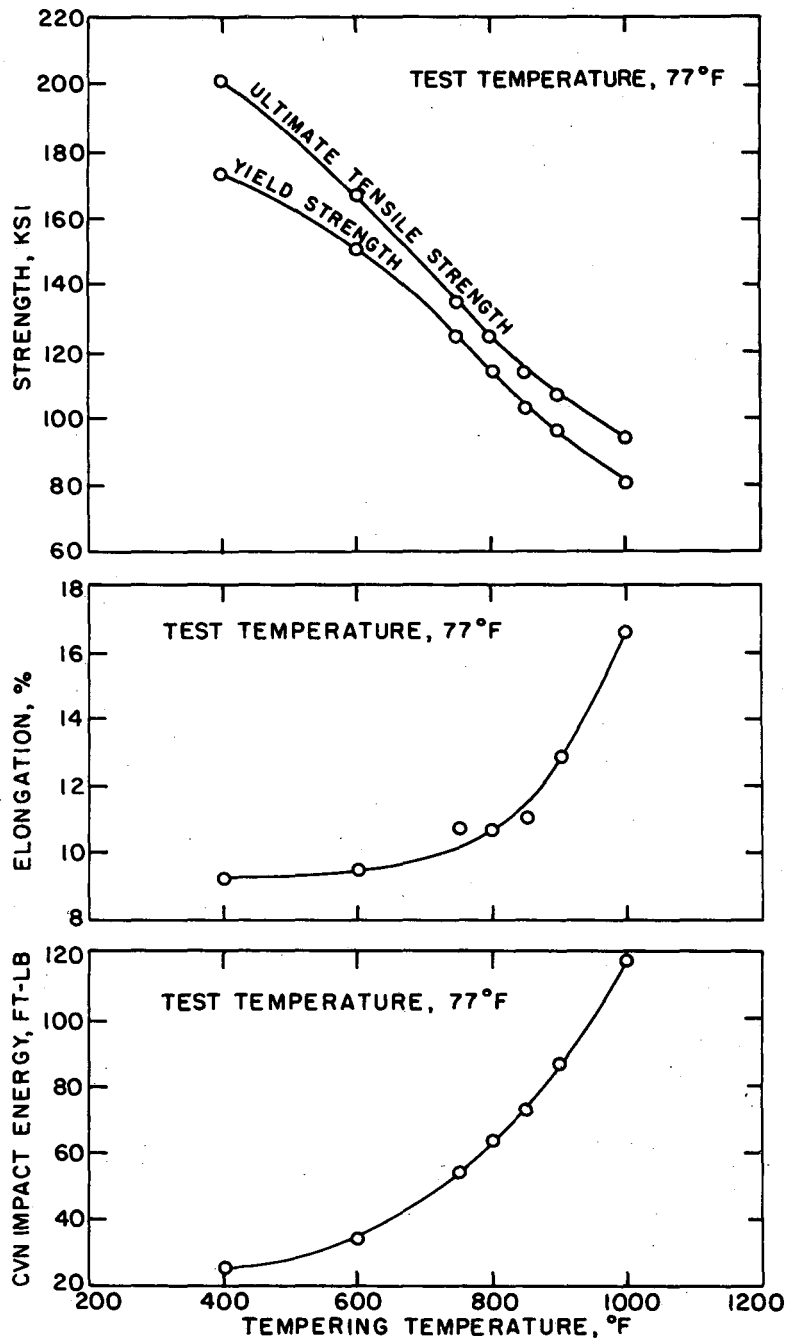

XBL 698-1308

Fig. 2

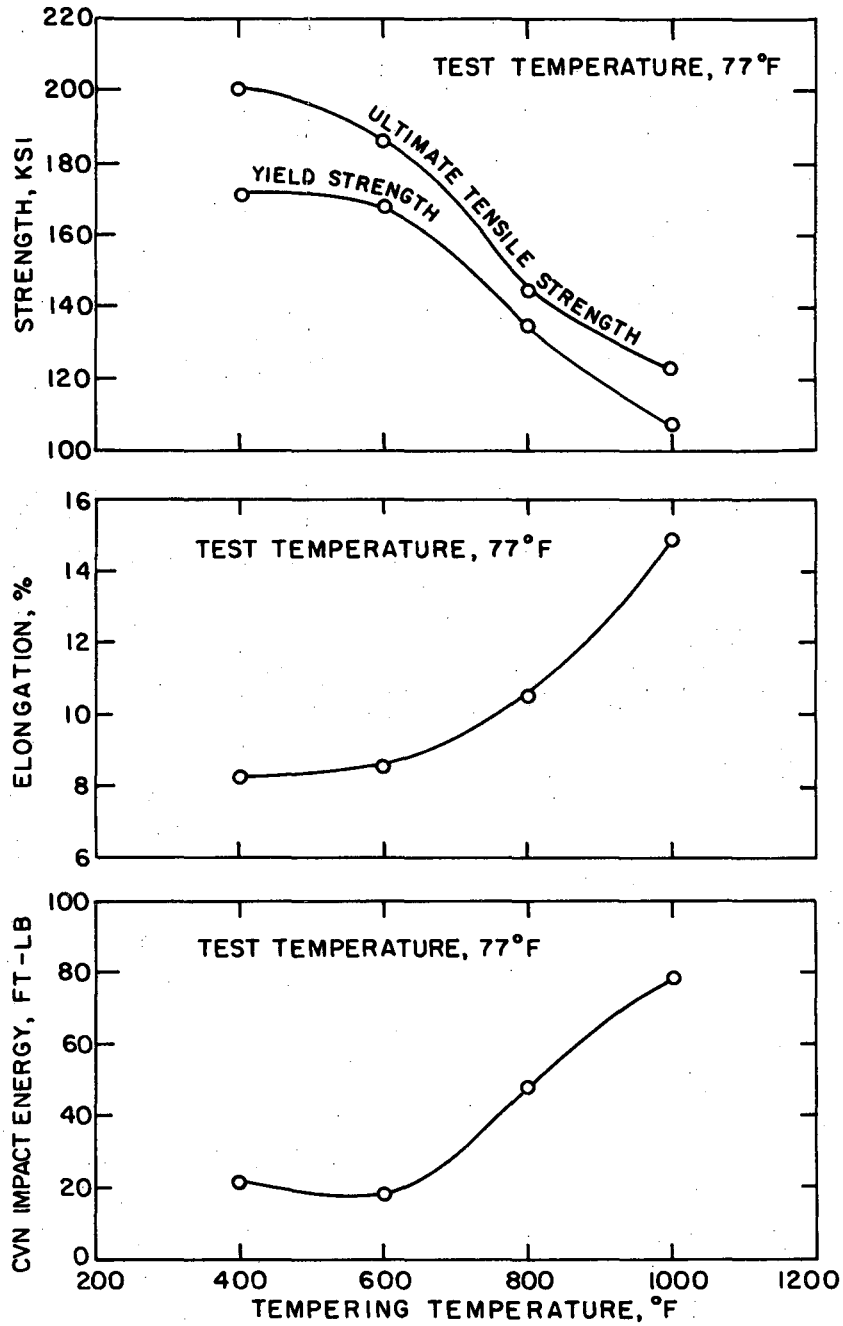

XBL 698-1307

Fig. 3

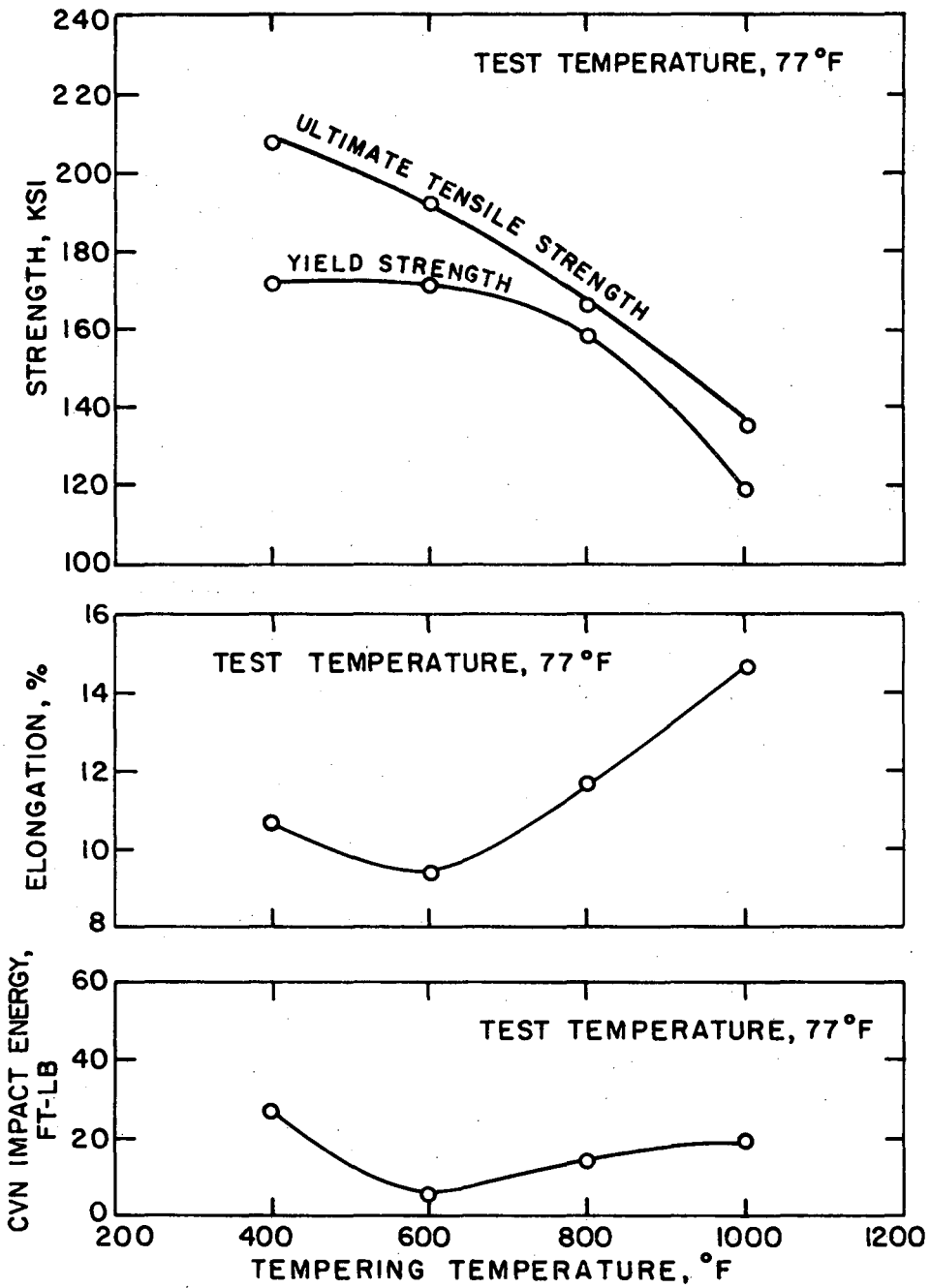

XBL 698-1306

Fig. 4

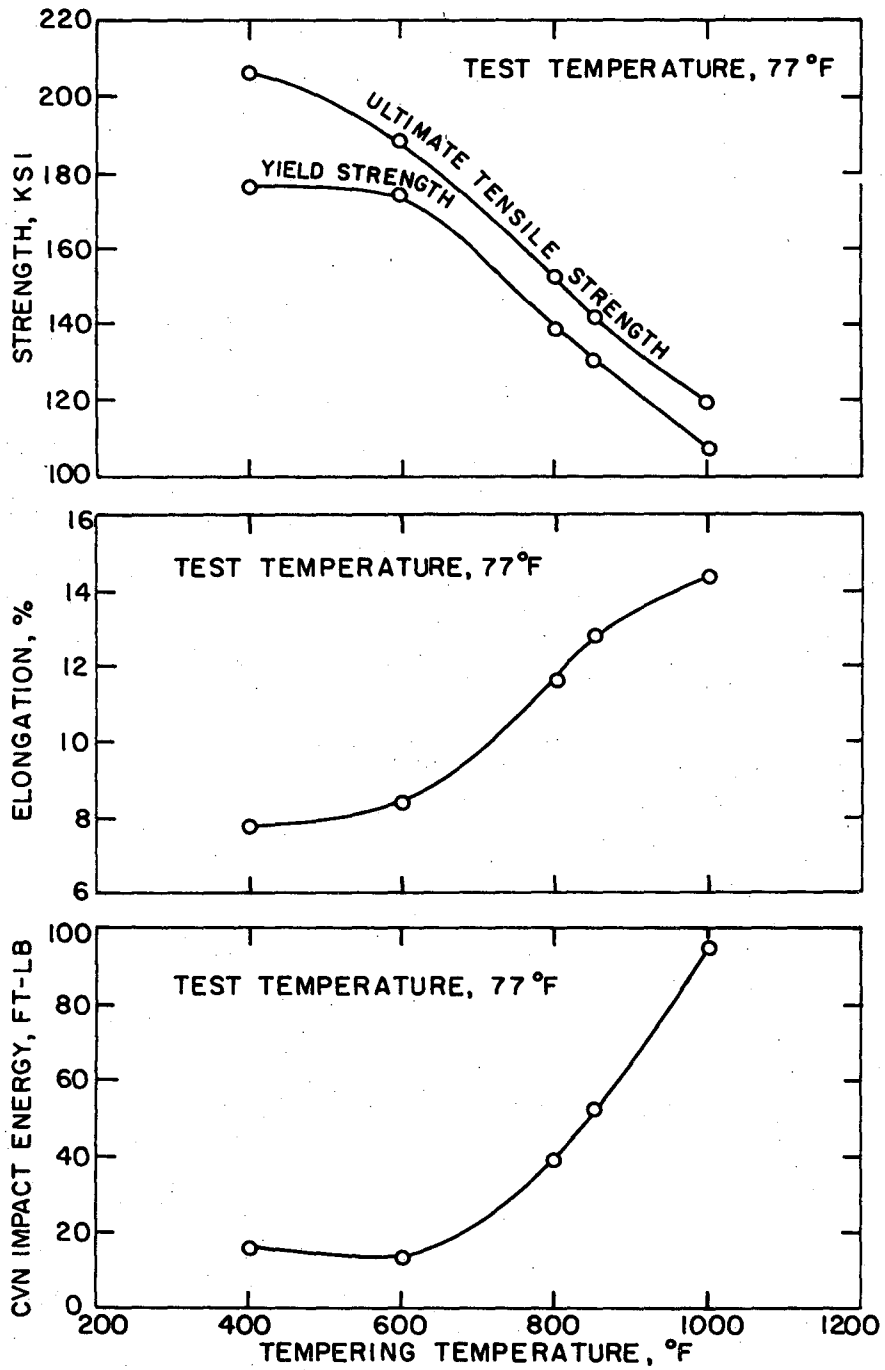

XBL 698-1305

Fig. 5

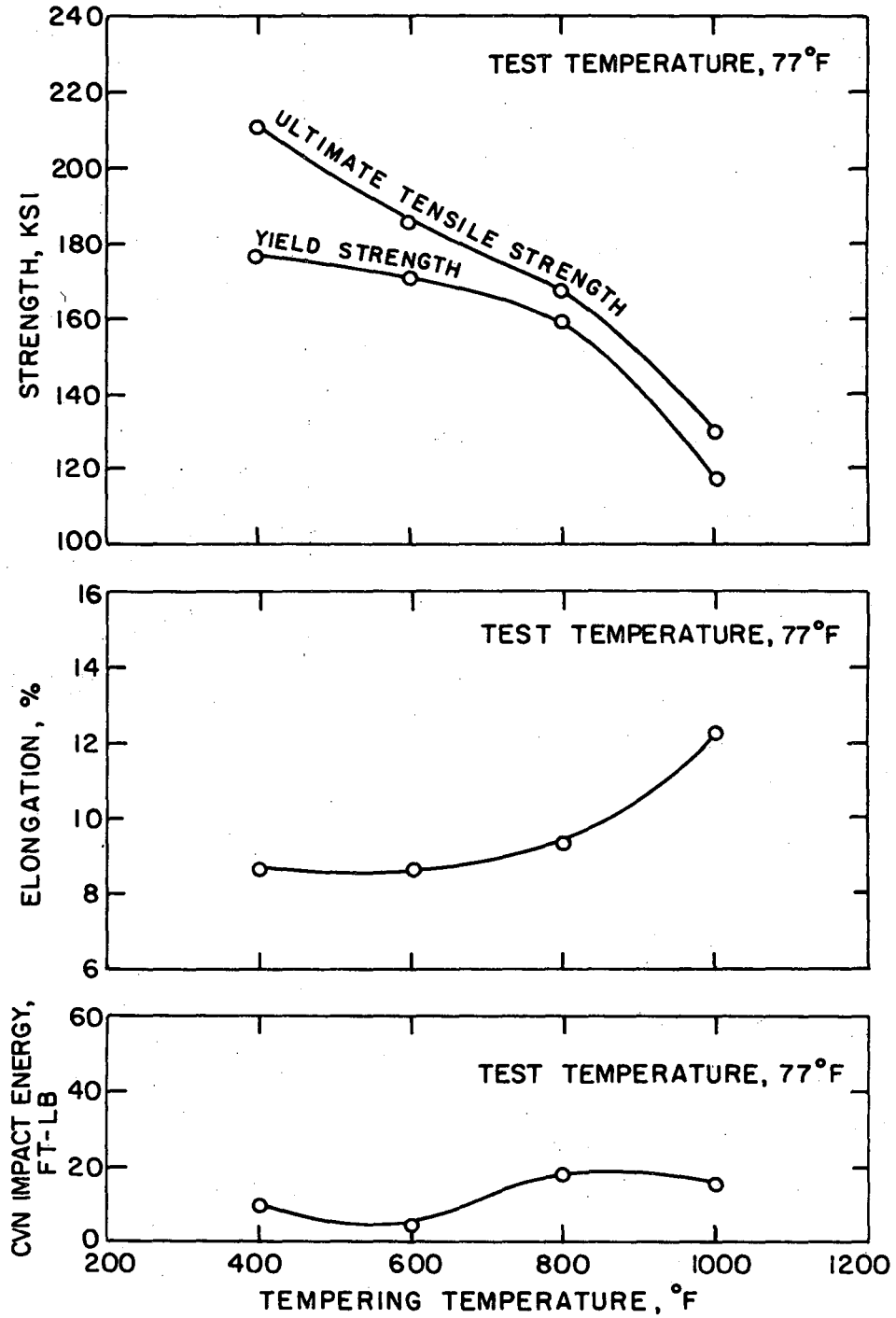

XBL 698-1303

Fig. 6

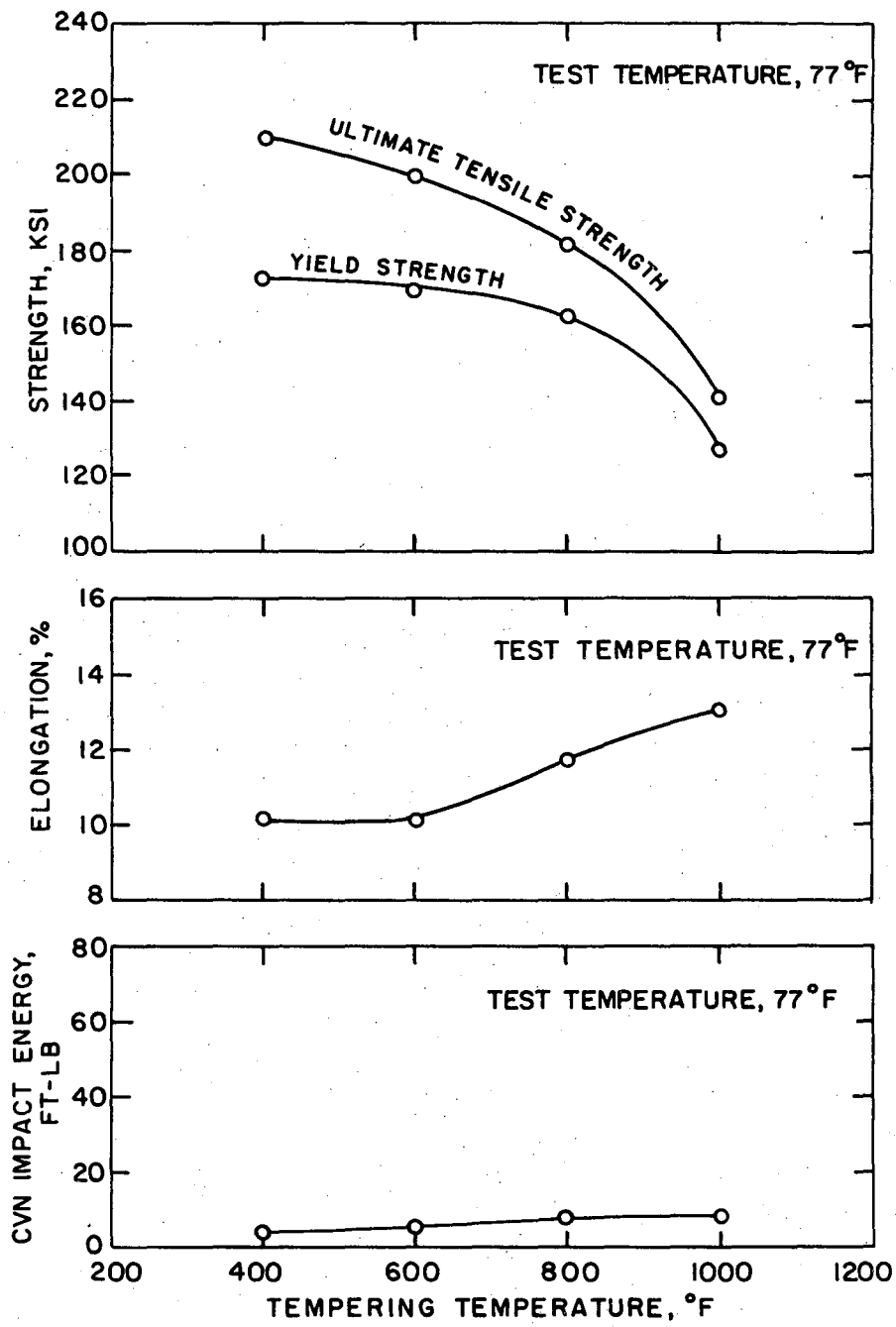

XBL 698-1304

Fig. 7

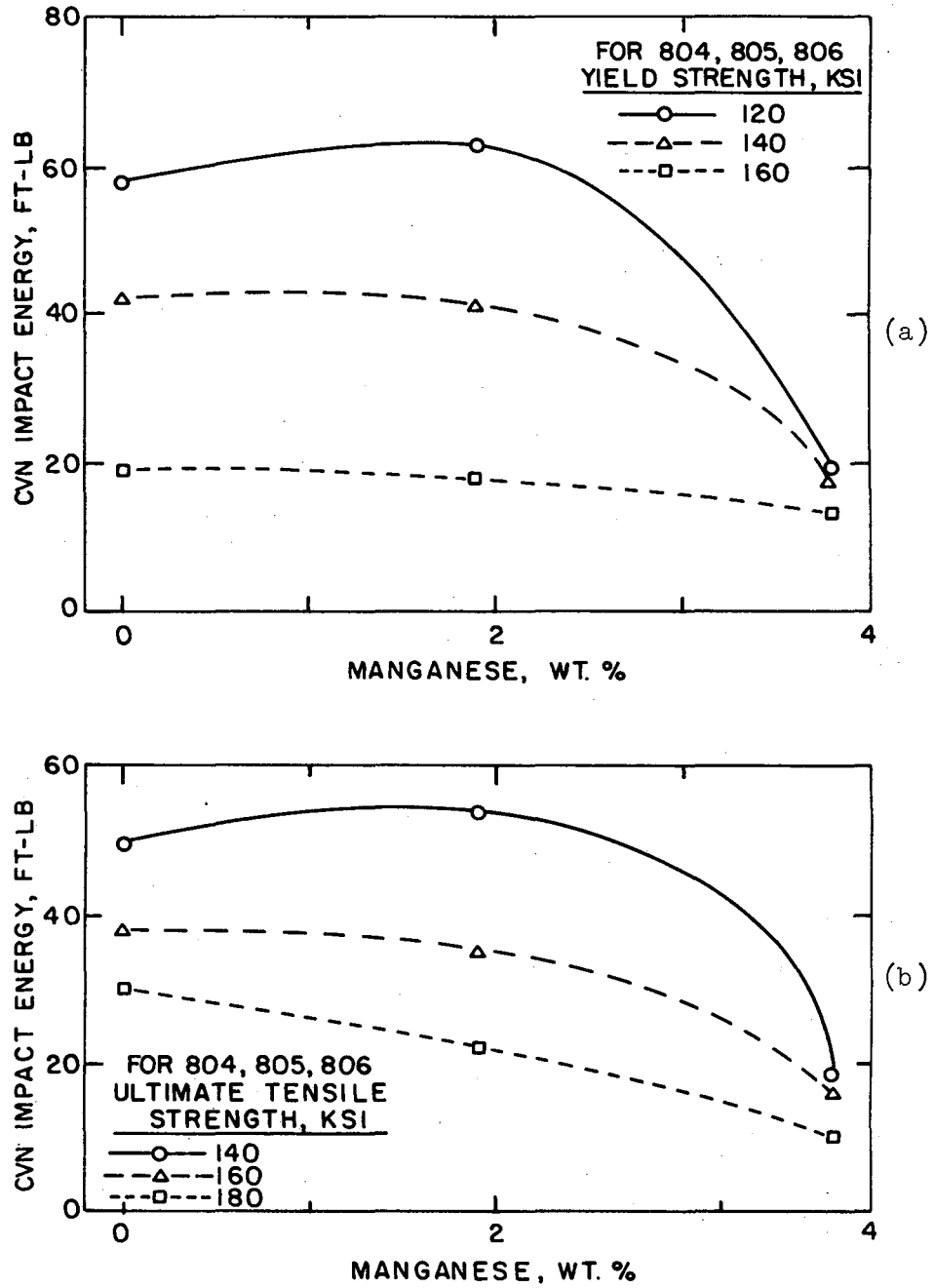

XBL 698-1310

Fig. 8

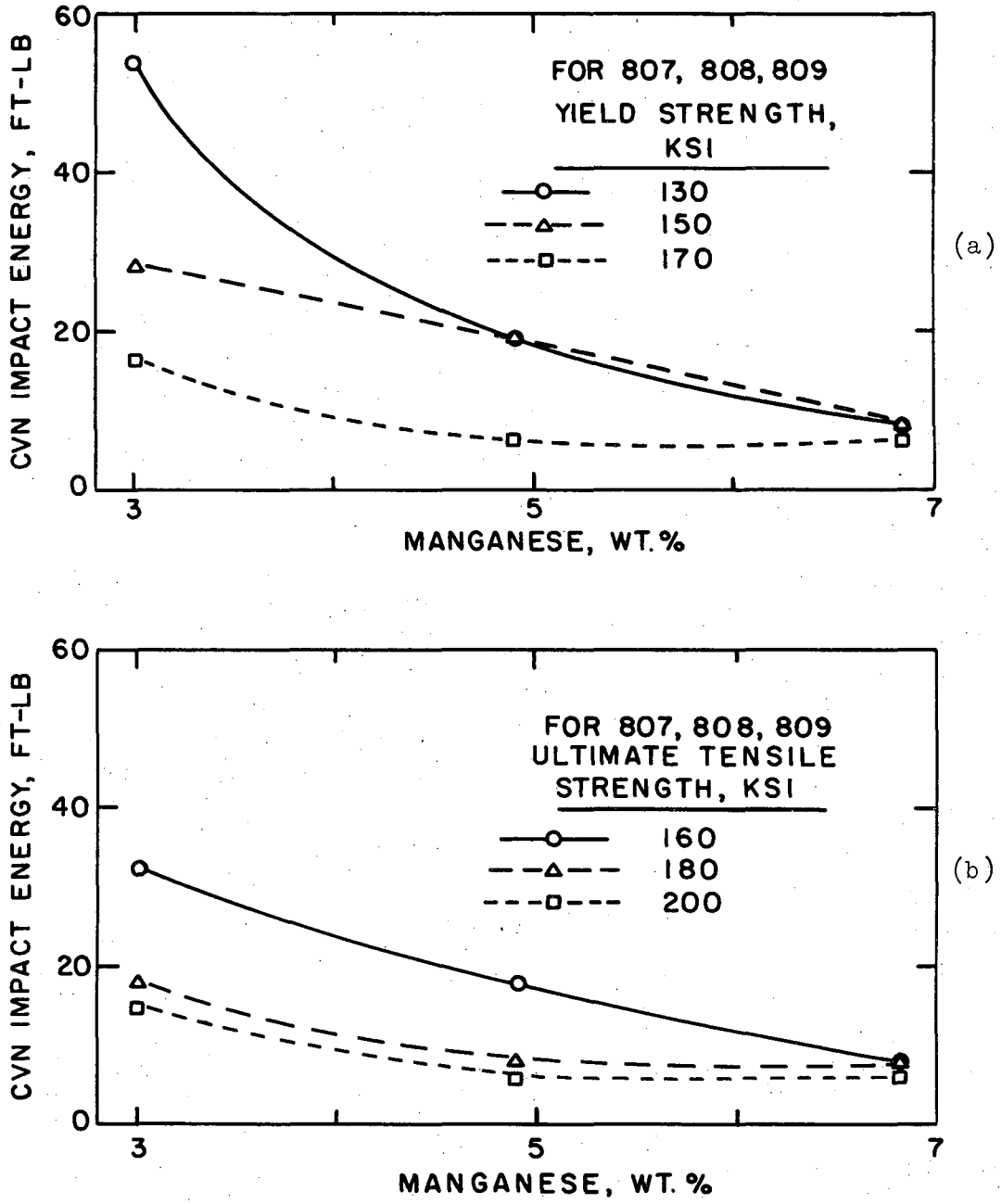

XBL 698-1309

Fig. 9

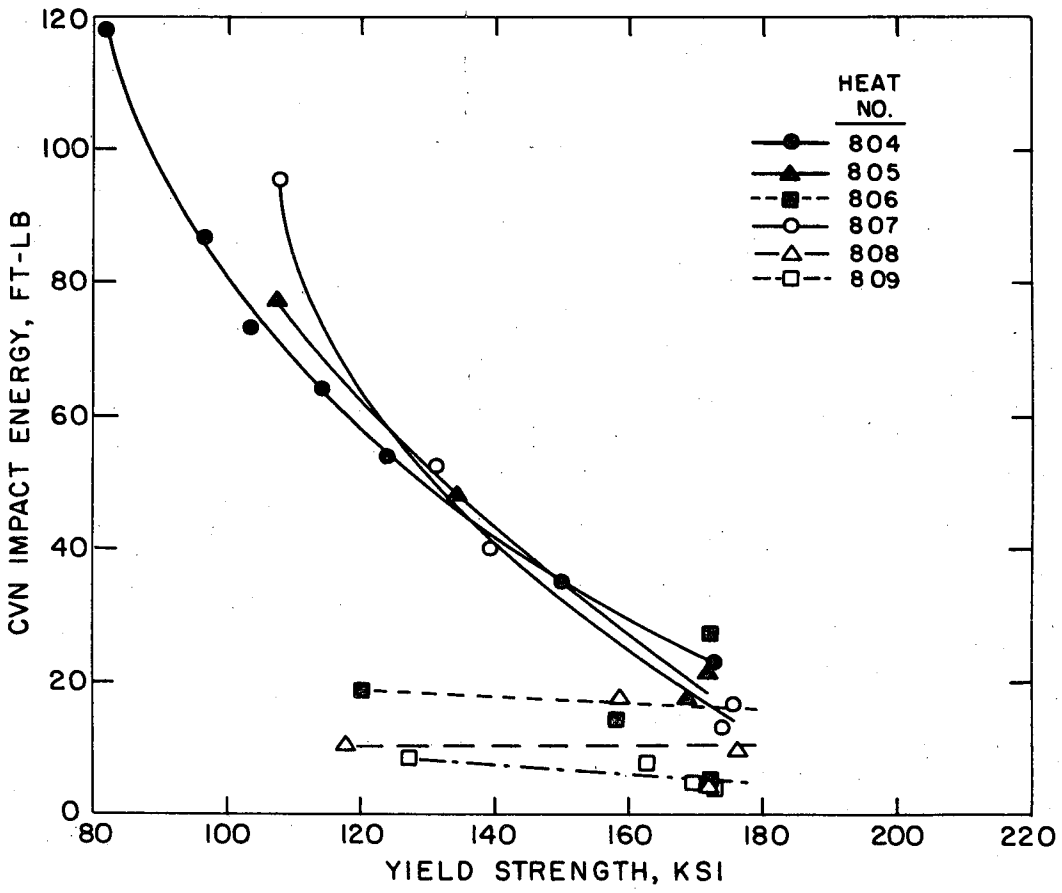

XBL 698-1313

Fig. 10

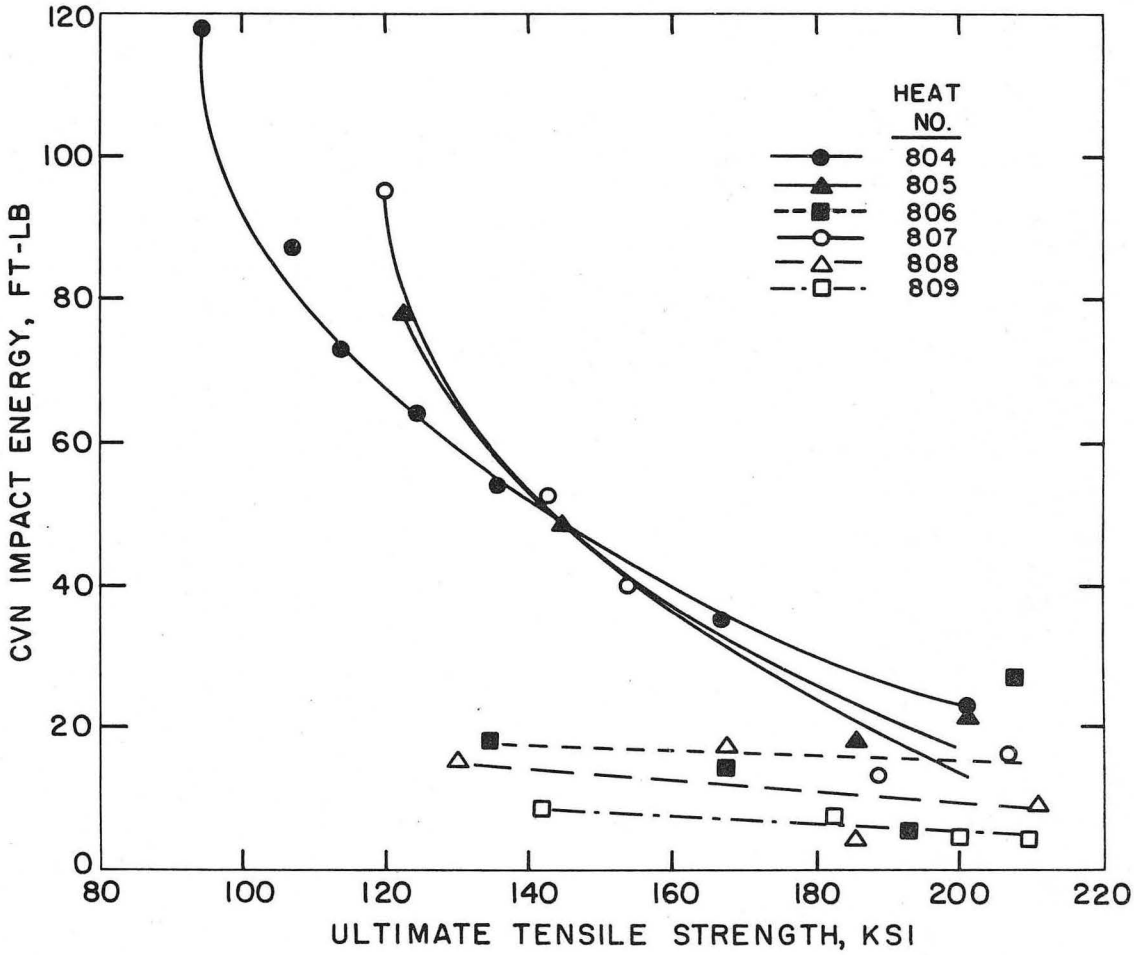

XBL 698-1312

Fig. 11

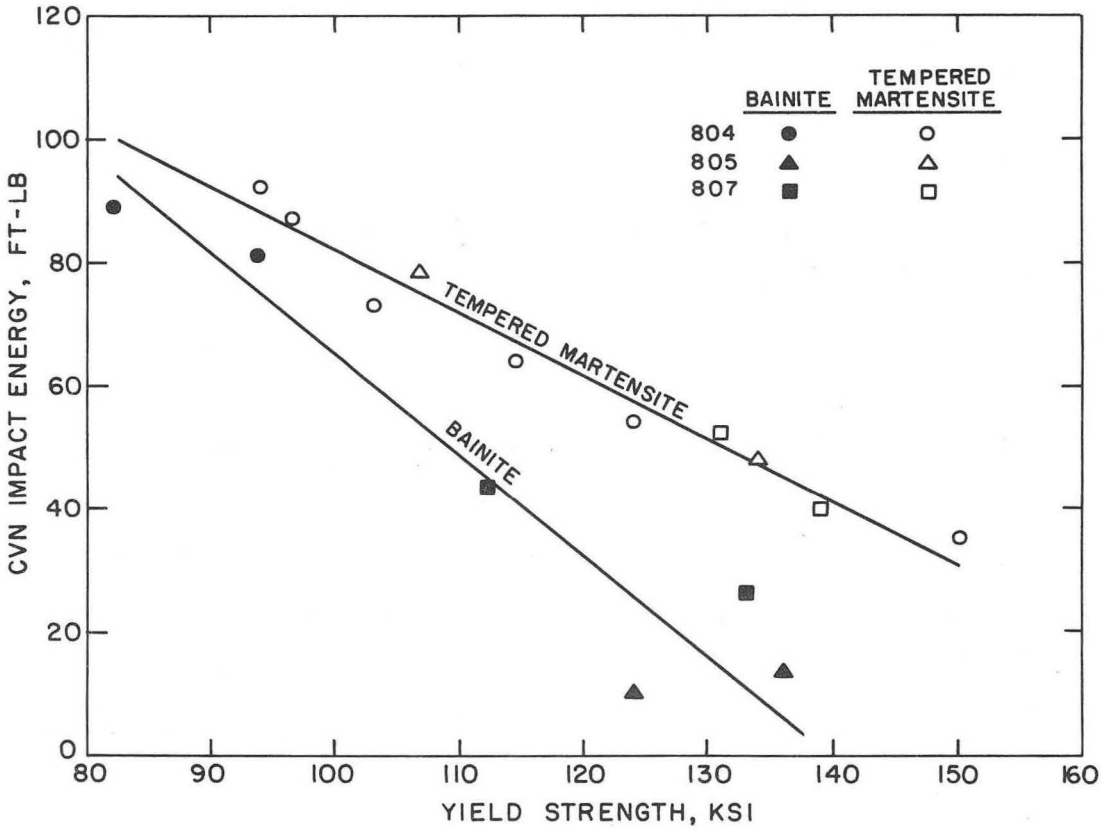

XBL 698-1311

Fig. 12

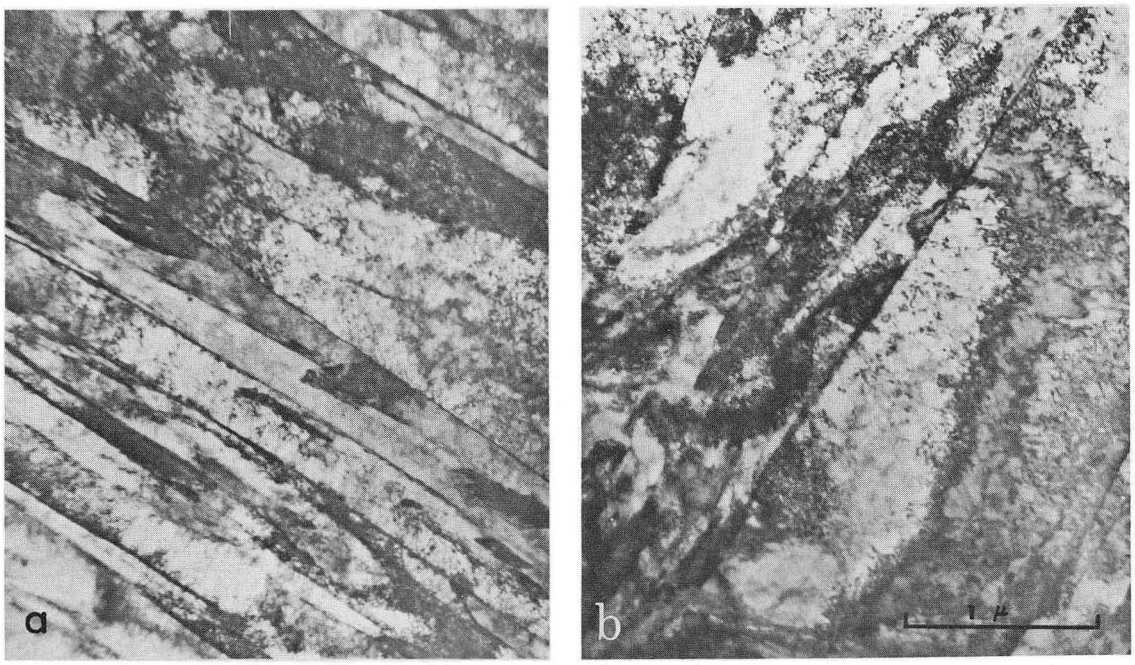

XBB 698-5564-A

Fig. 13

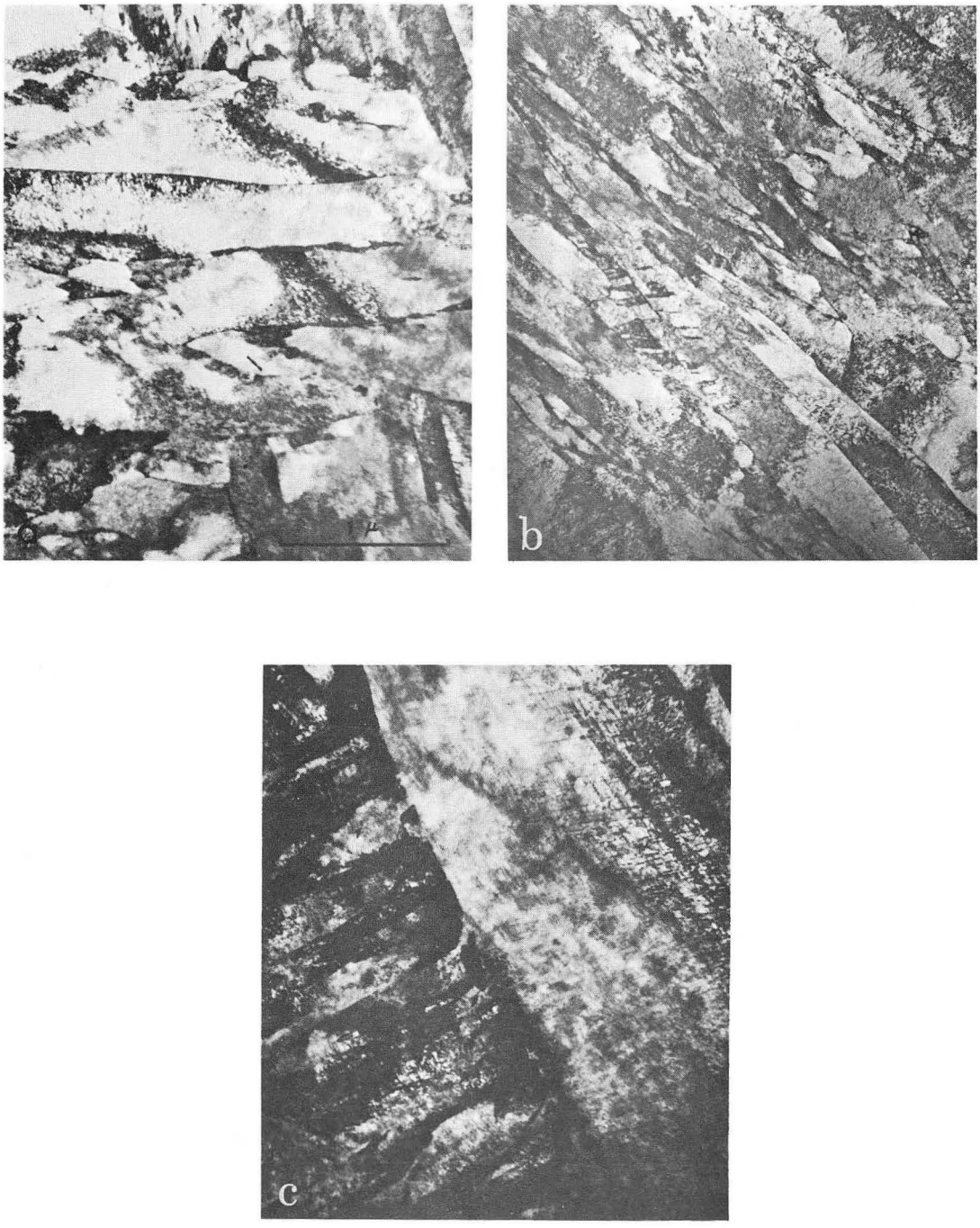

XBB 698-5583-A

Fig. 14

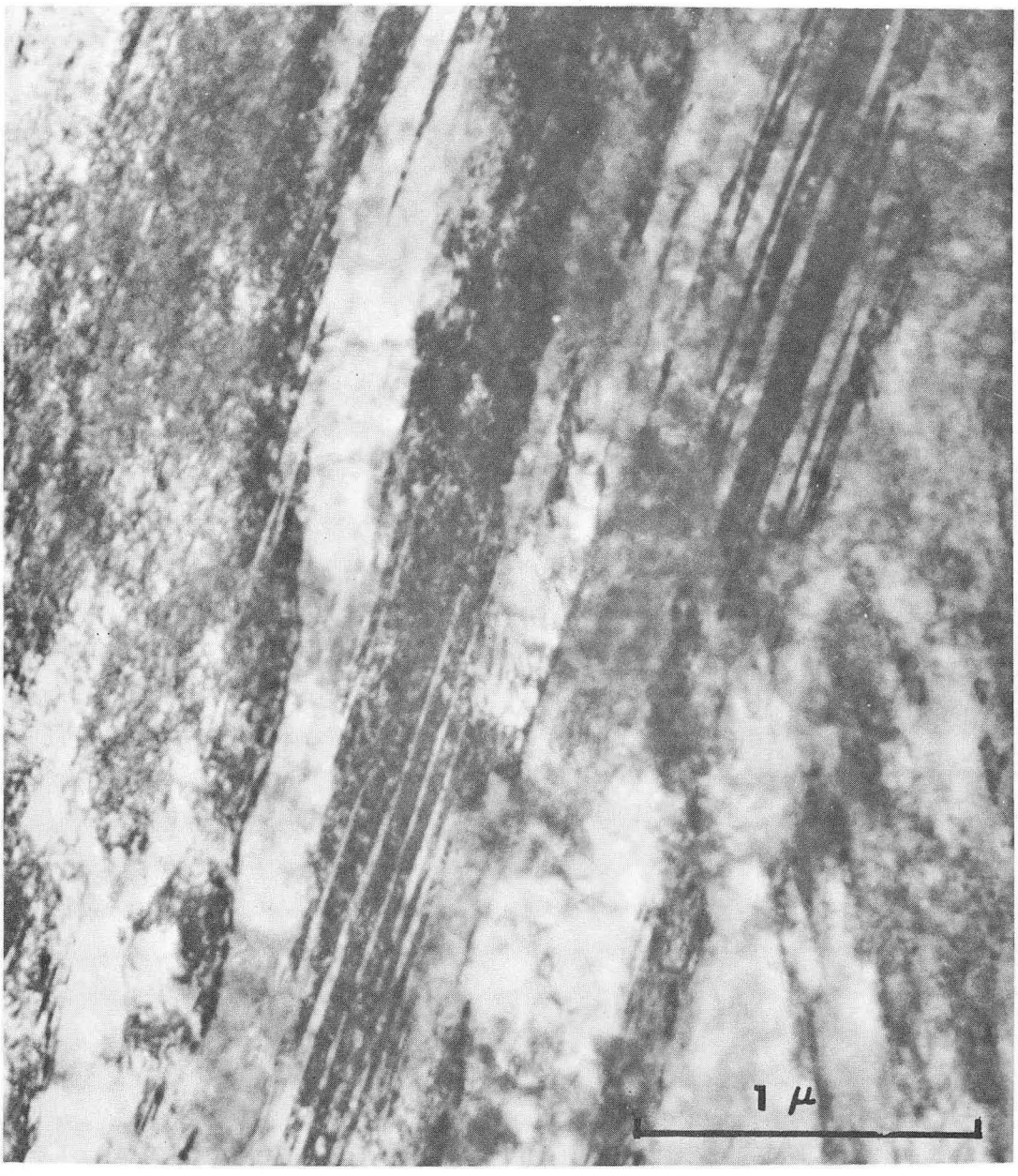

XBB 698-5573

Fig. 15

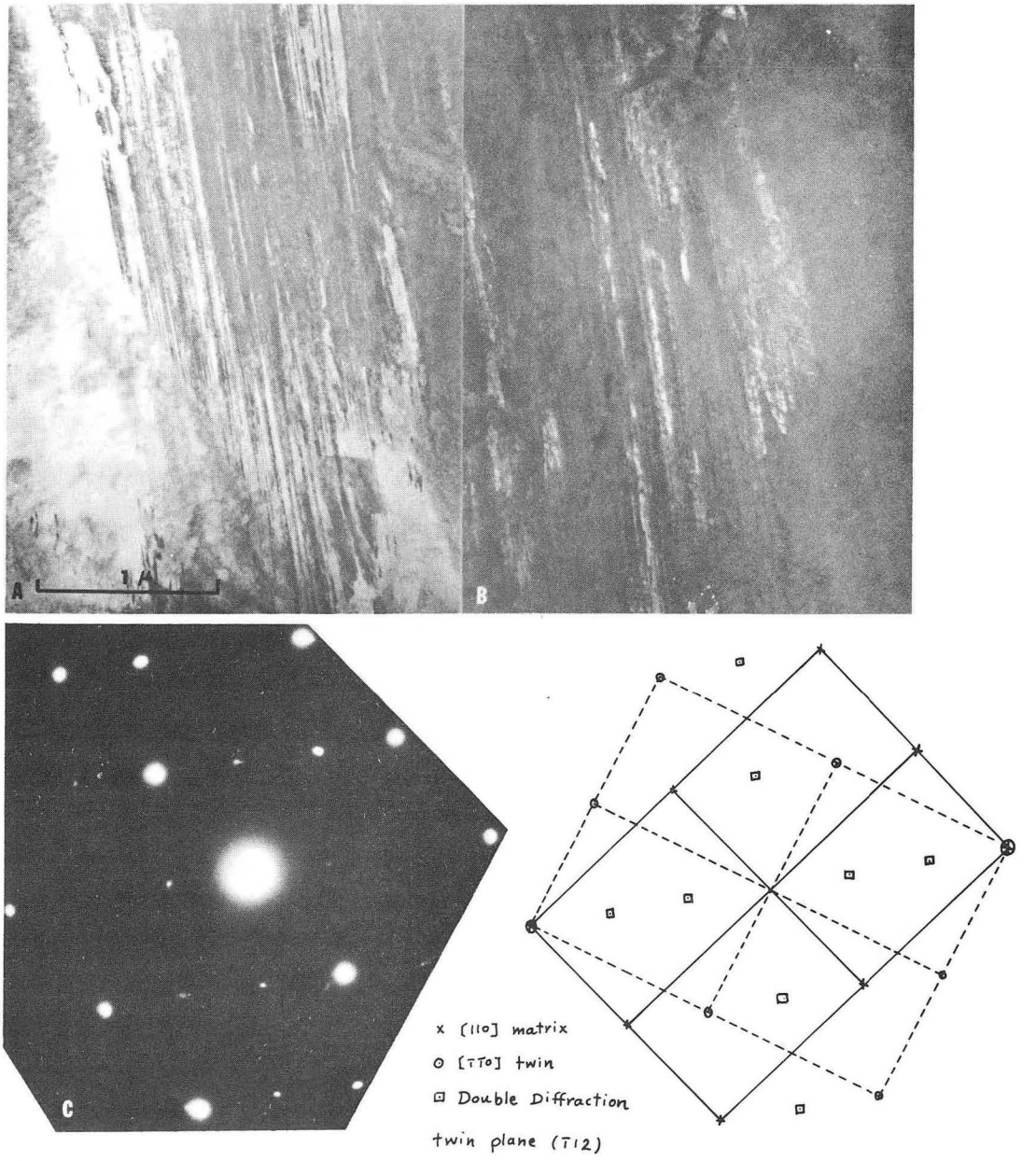

XBB 698-5554

Fig. 16

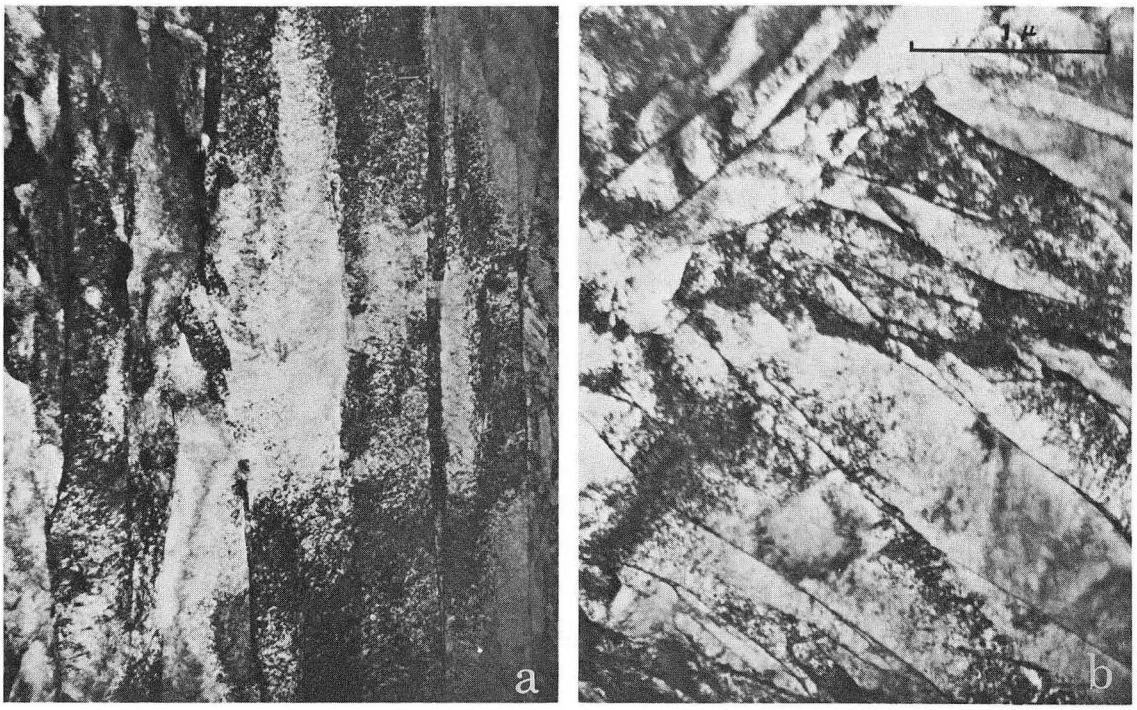

XBB 698-5556-A

Fig. 17

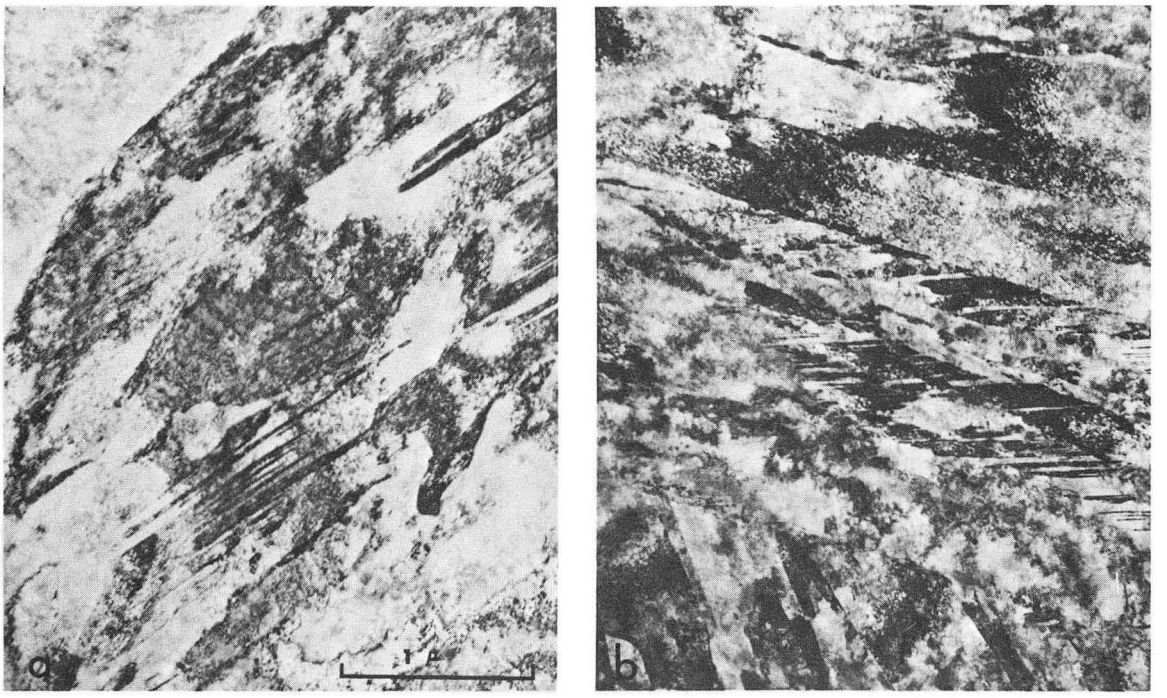

XBB 698-5555-A

Fig. 18

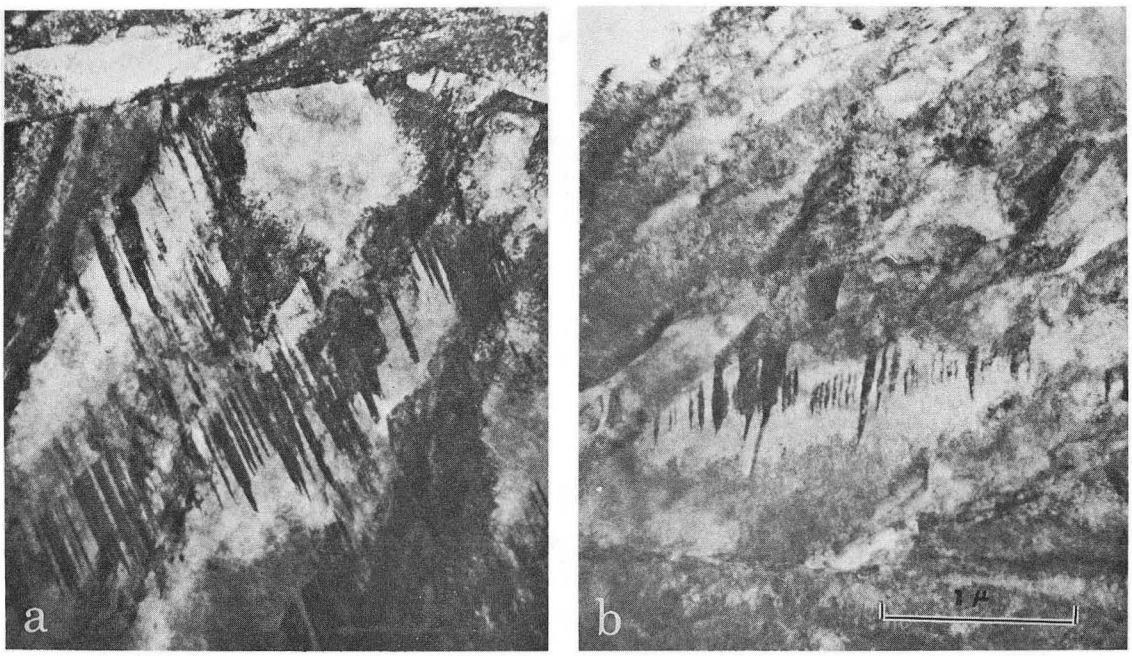

XBB 698-5557-A

Fig. 19

XBB 698-5579-A

Fig. 19

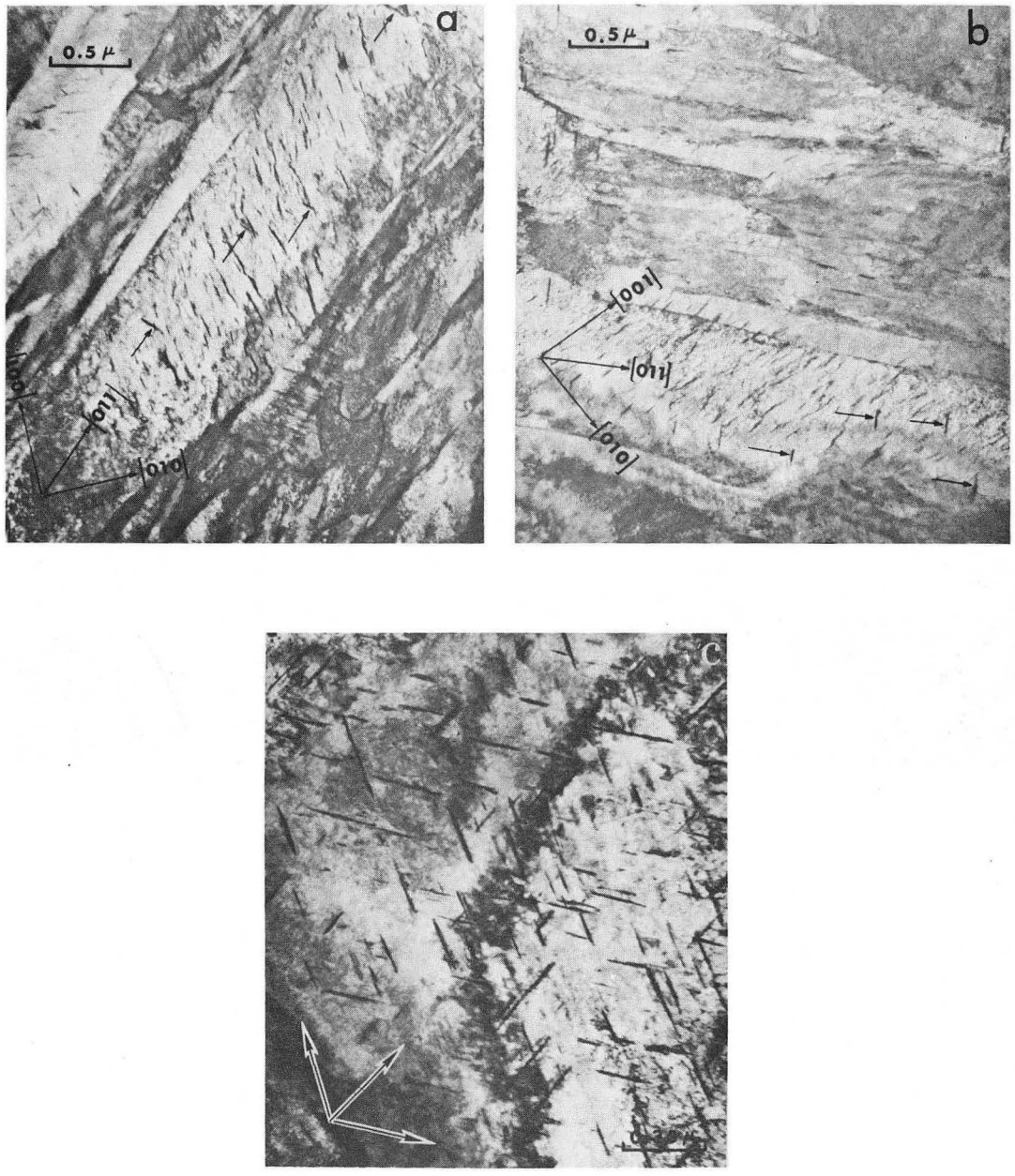

XBB 698-5582-A

Fig. 20

XBB 698-5581-A

Fig. 21

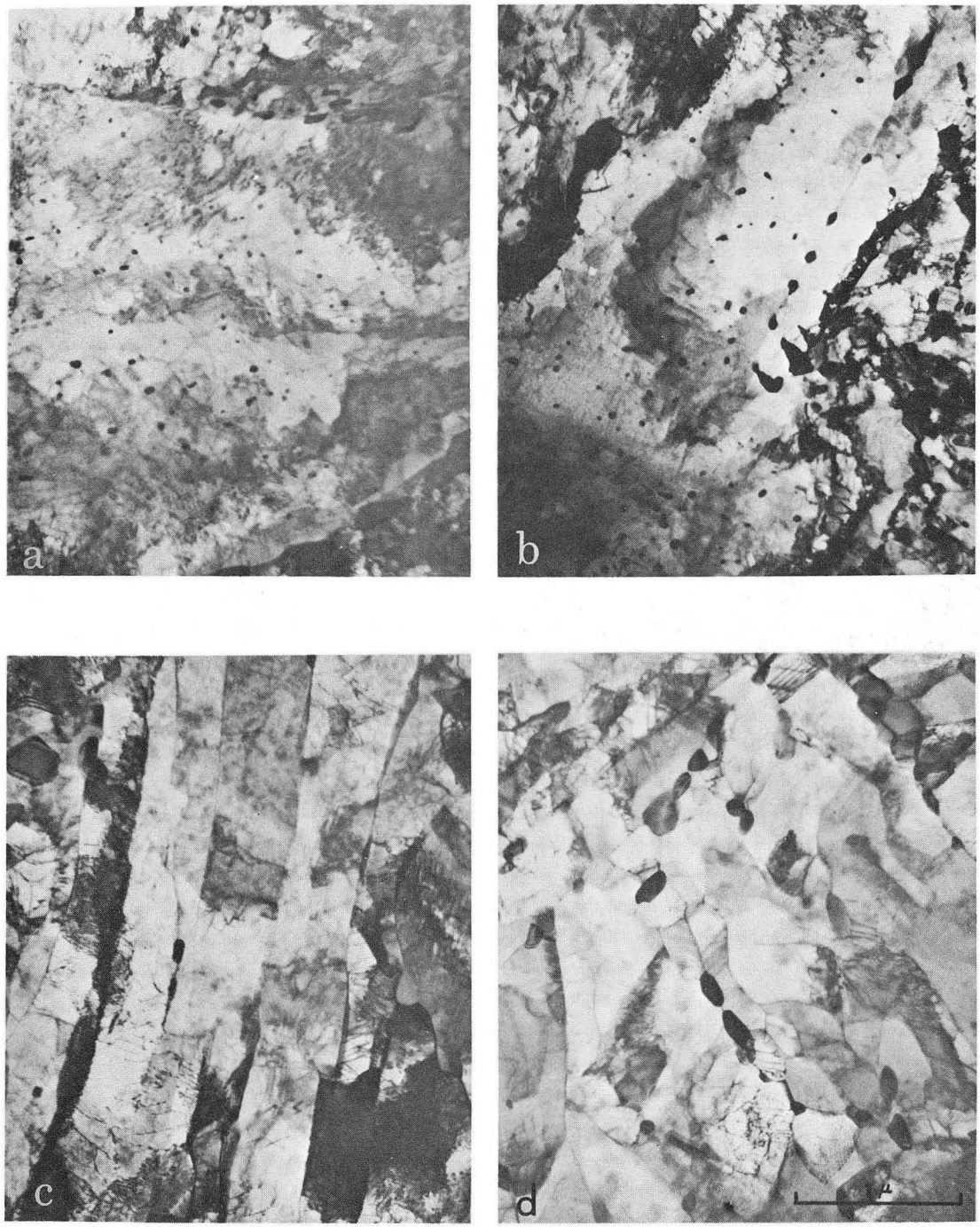

XBB 698-5569-A

Fig. 22

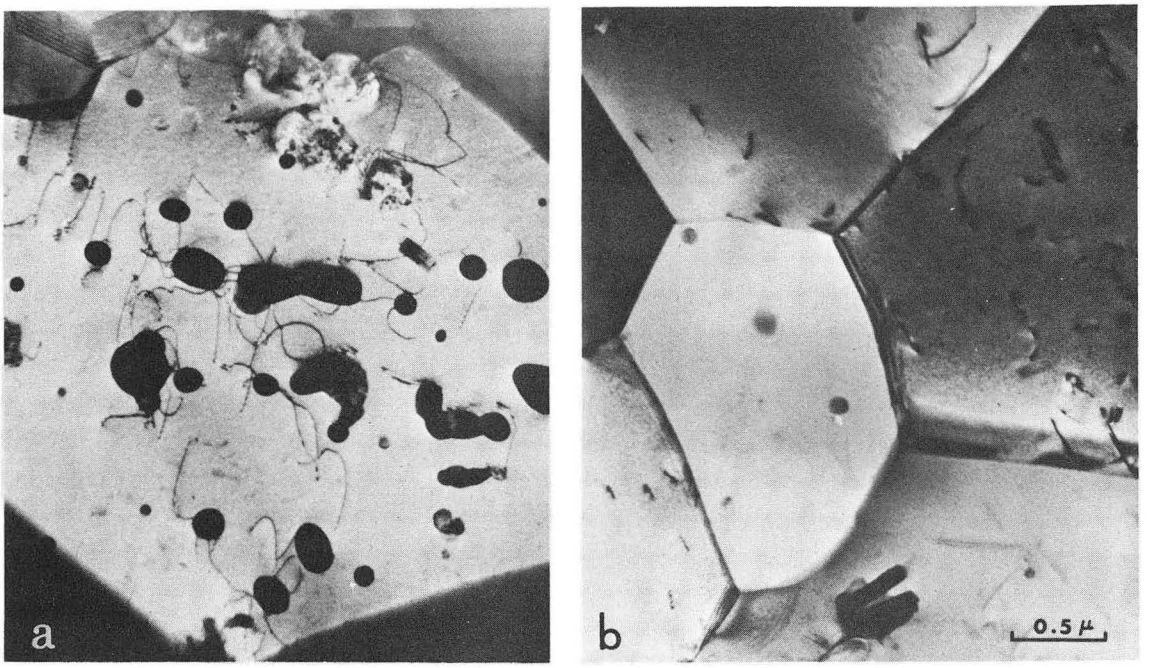

XBB 698-5563-A

Fig. 23

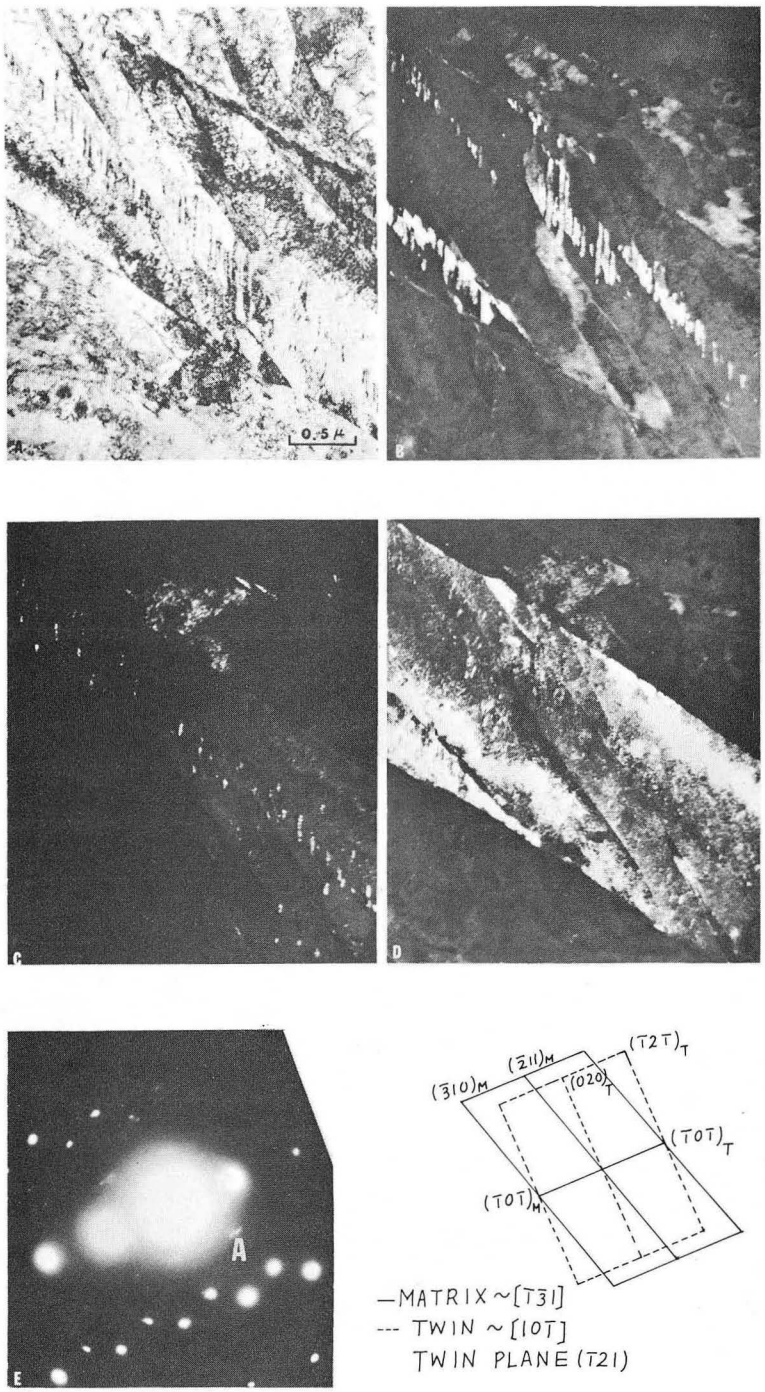

XBB 698-5553

Fig. 24

XBB 698-5577

Fig. 25

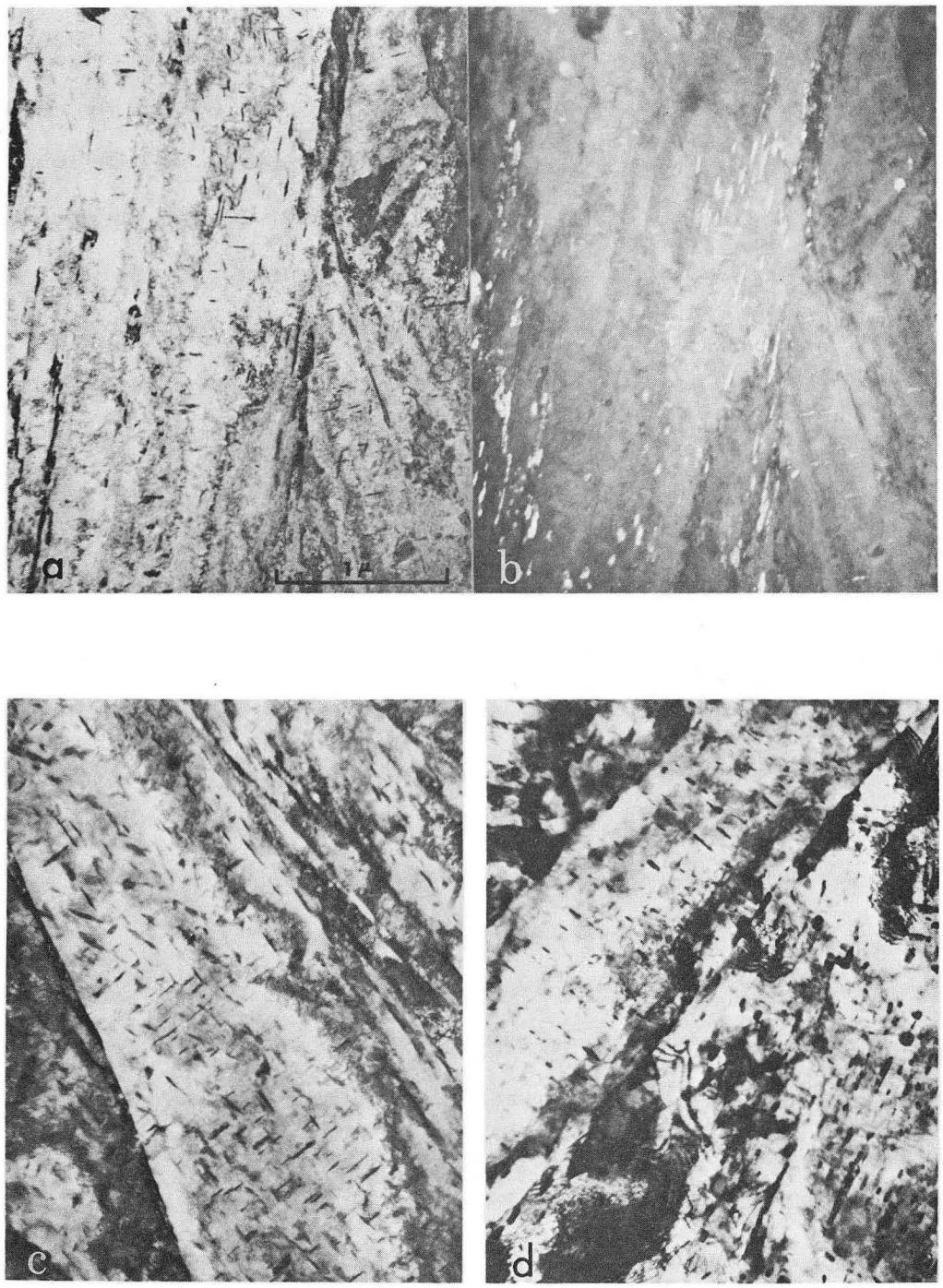

XBB 698-5568-A

Fig. 26

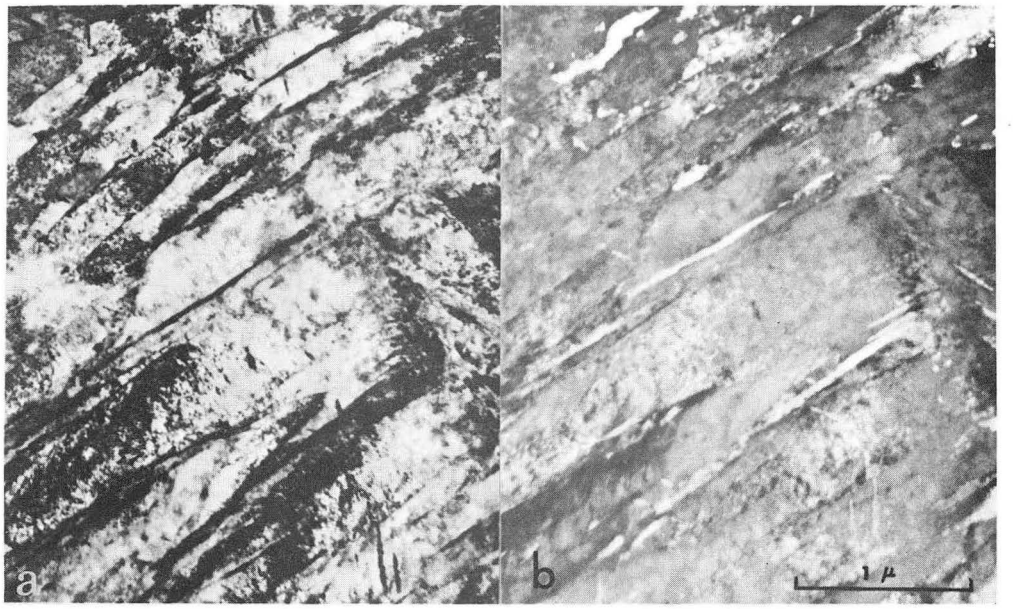

XBB 698-5567-A

Fig. 27

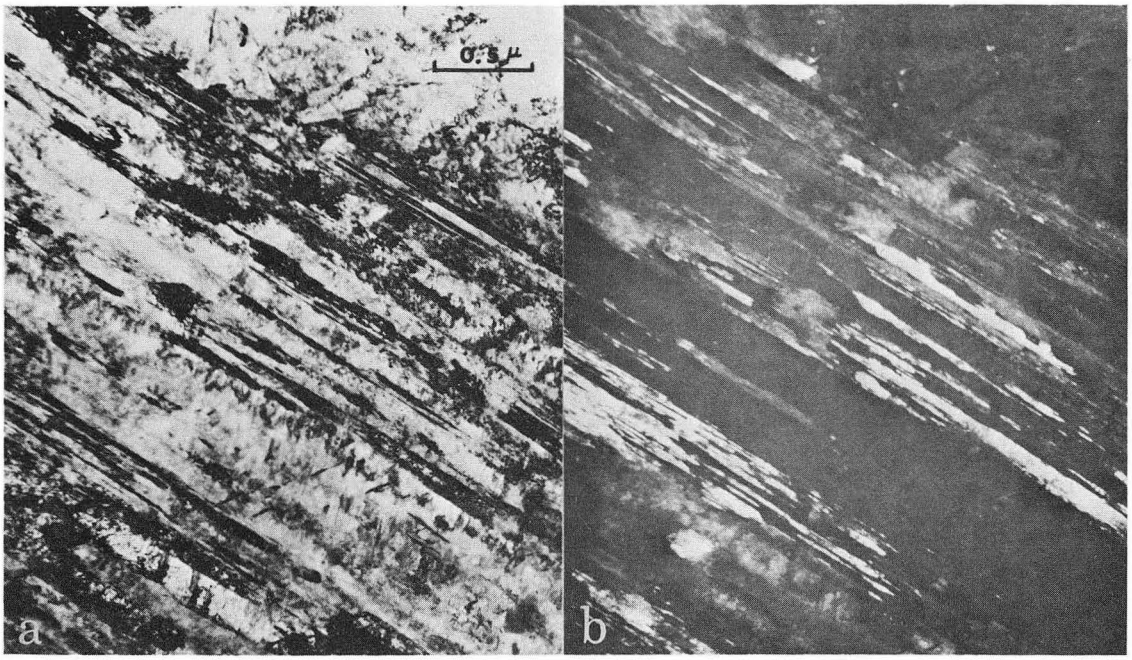

XBB 698-5558-A

Fig. 28

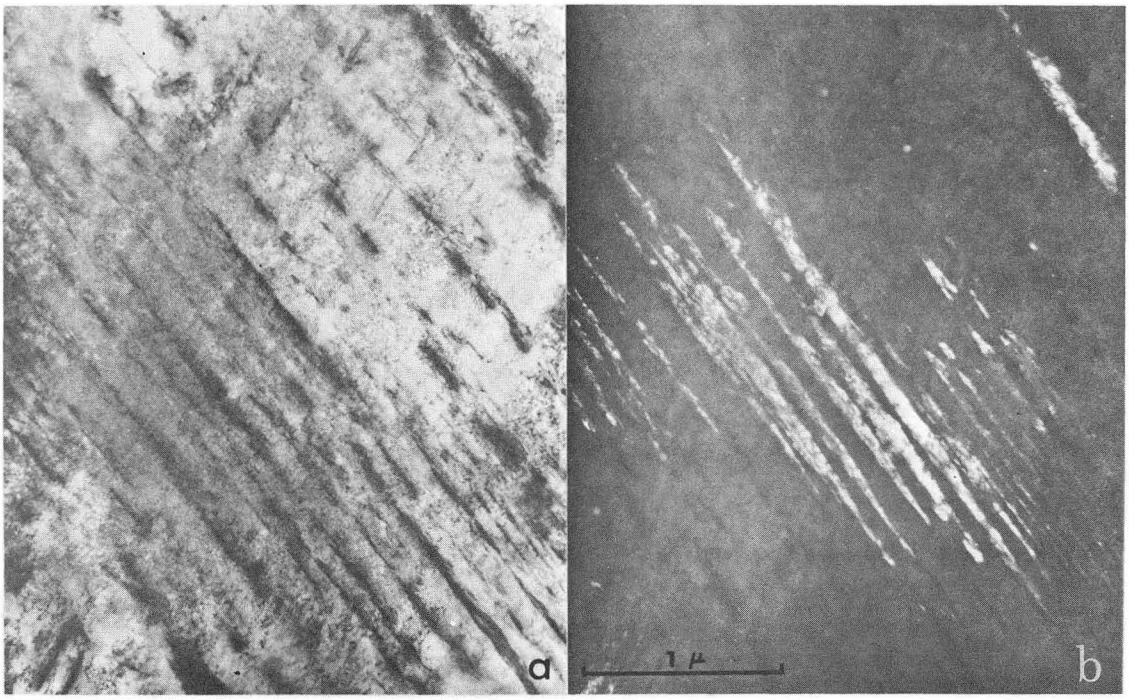

XBB 698-5584-A

Fig. 29

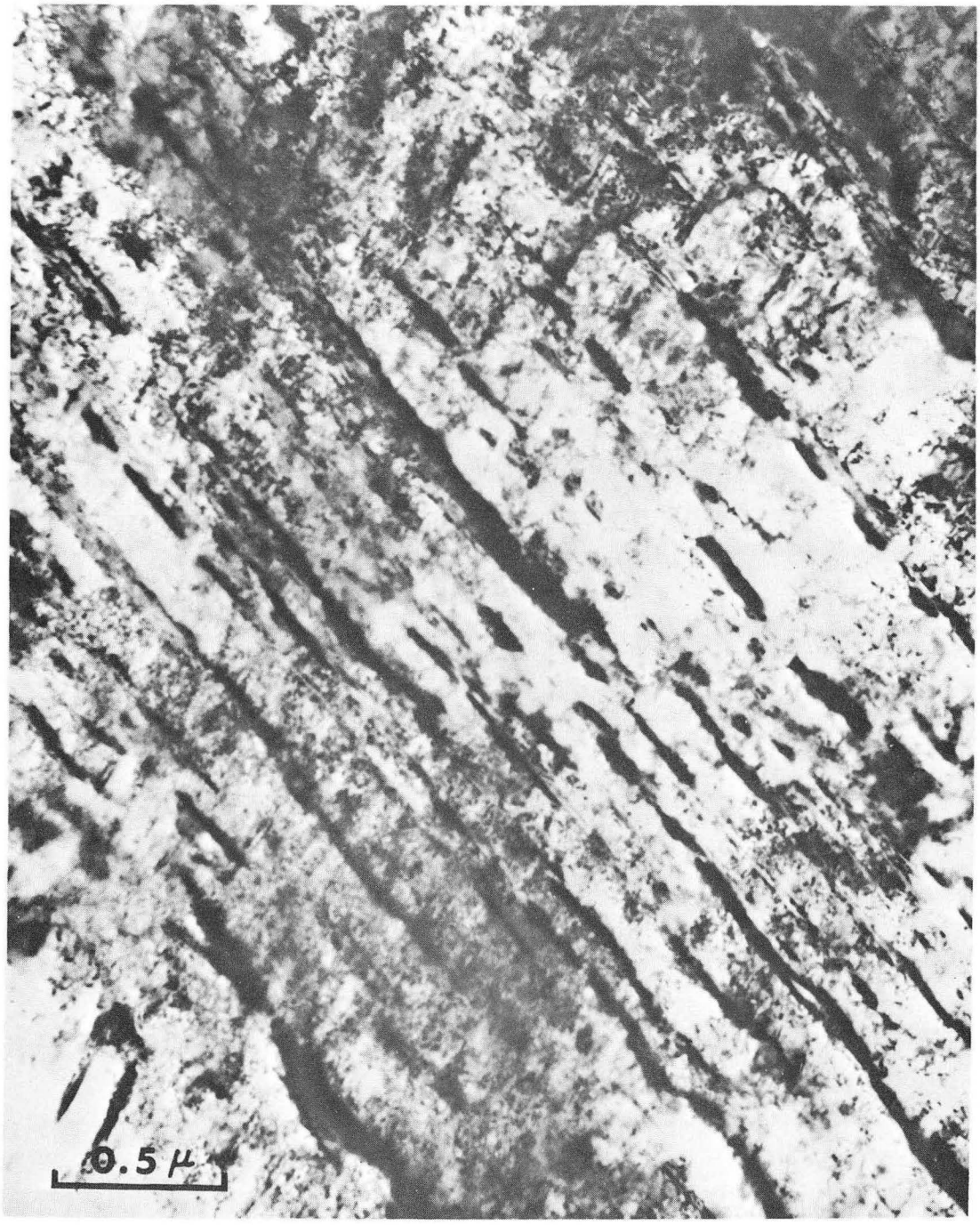

XBB 698-5576

Fig. 30

XBB 698-5574

Fig. 31

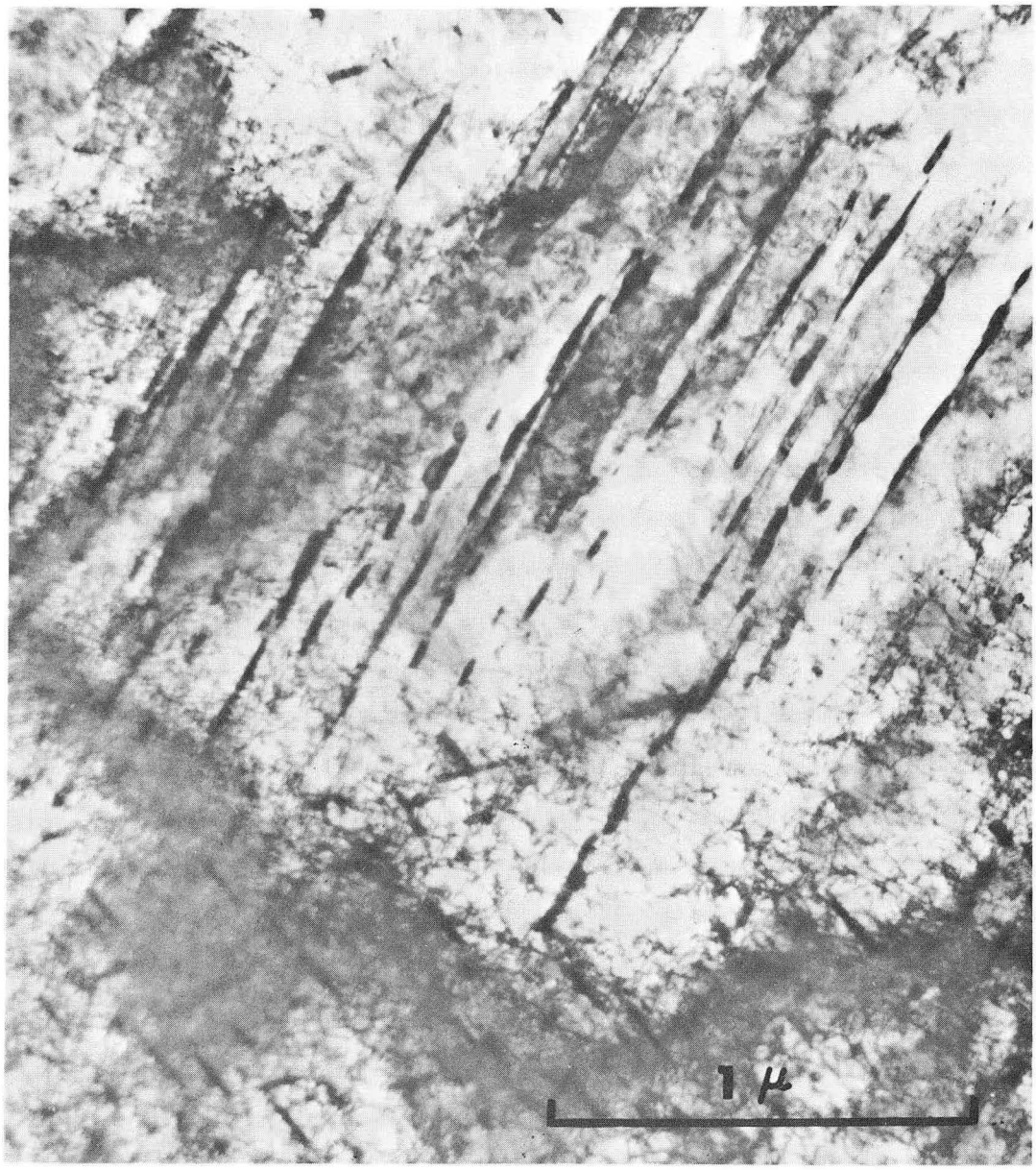

XBB 698-5578

Fig. 32

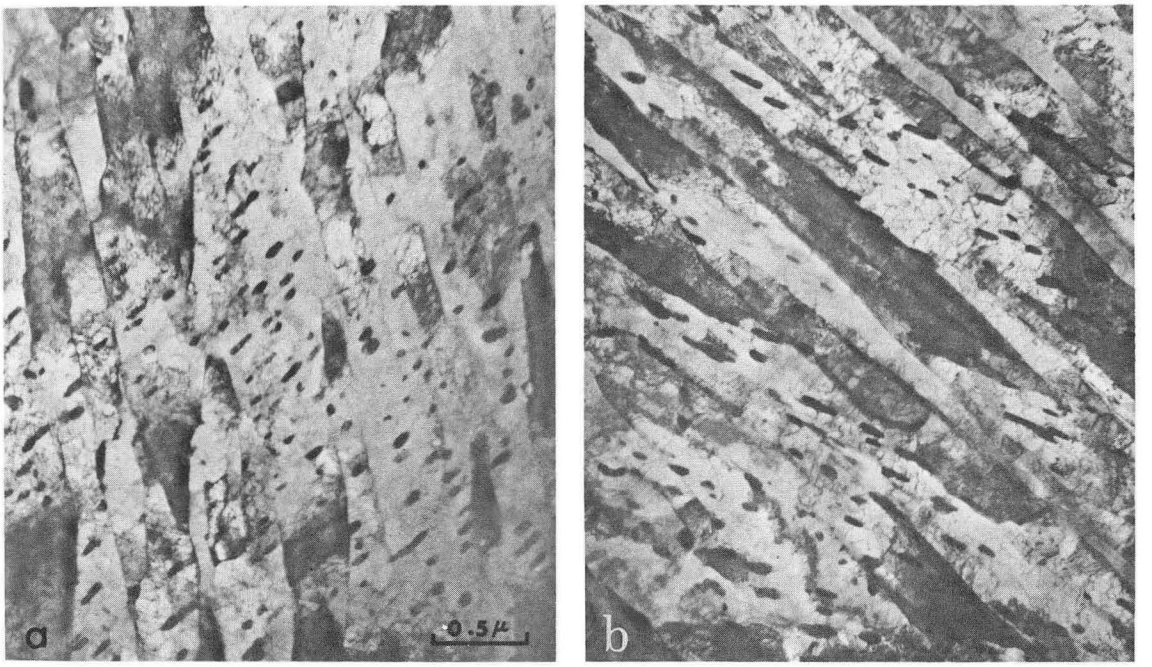

XBB 698-5561-A

Fig. 33

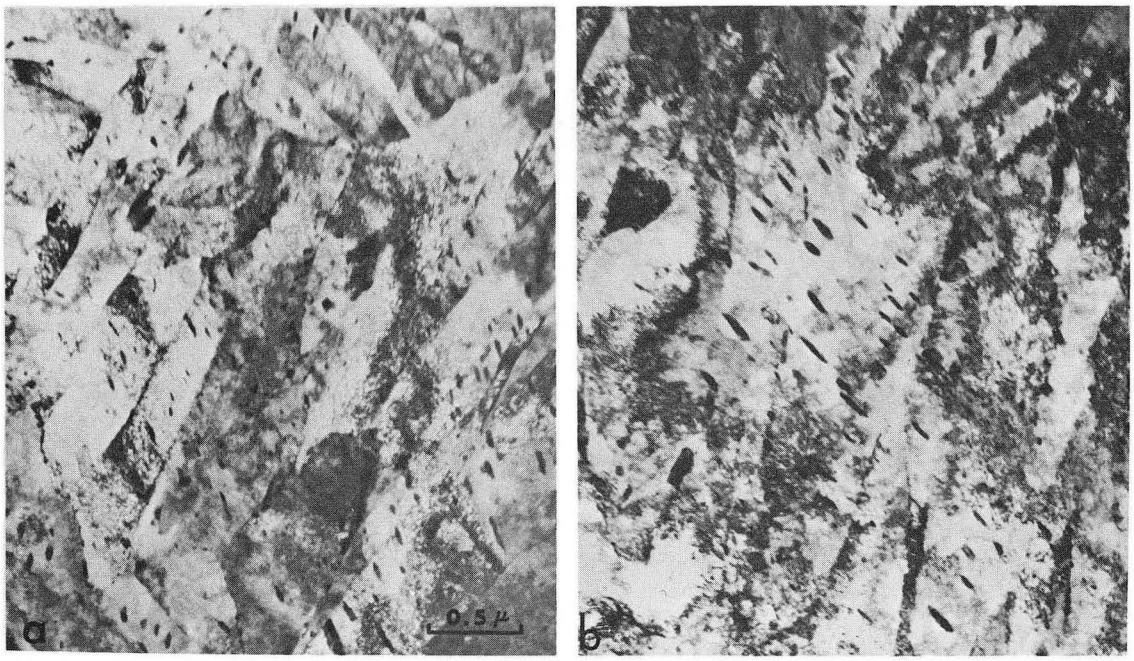

XBB 698-5562-A

Fig. 34

XBB 698-5575

Fig. 35

XBB 698-5572

Fig. 36

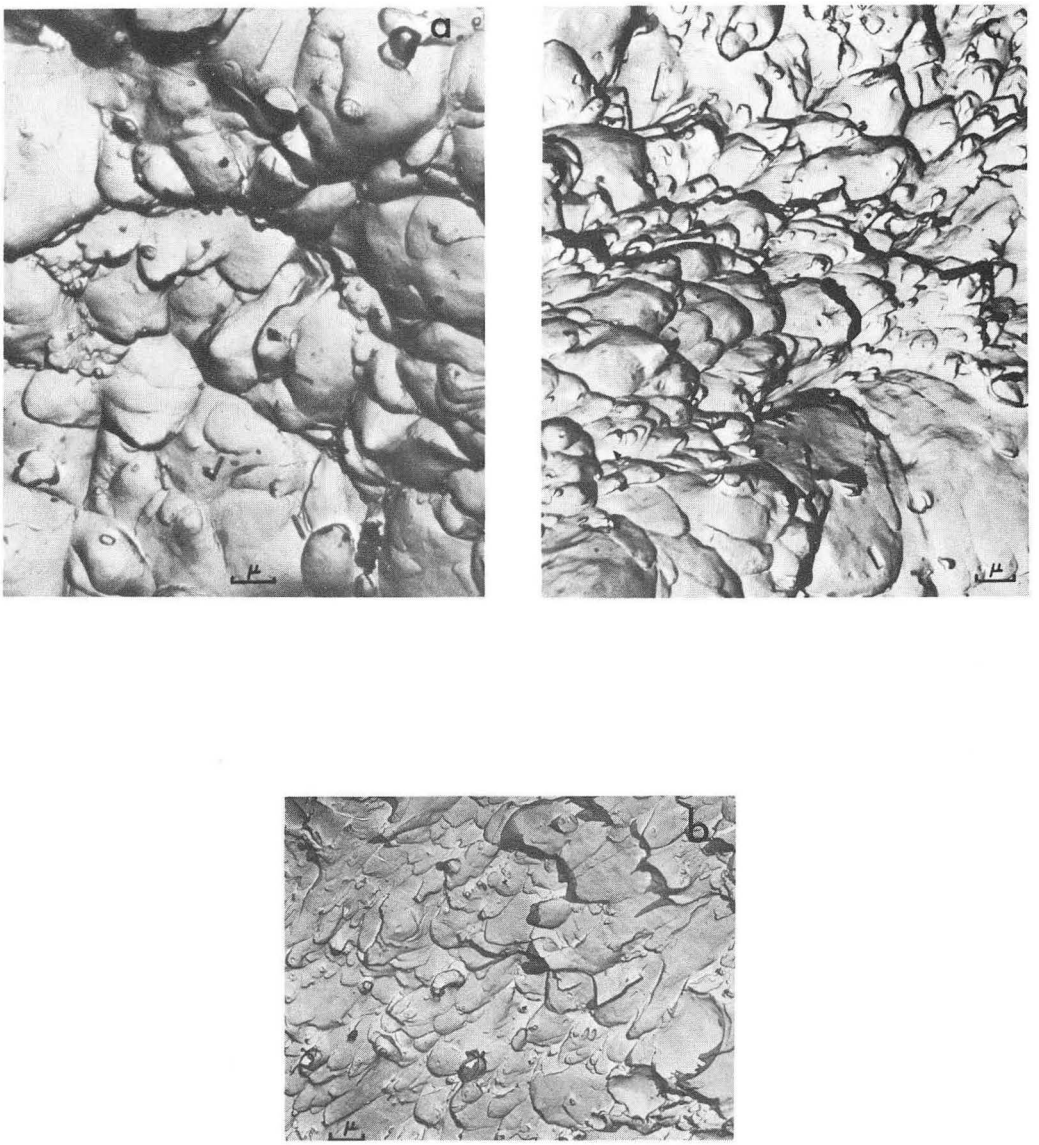

XBB 698-5586-A

Fig. 37

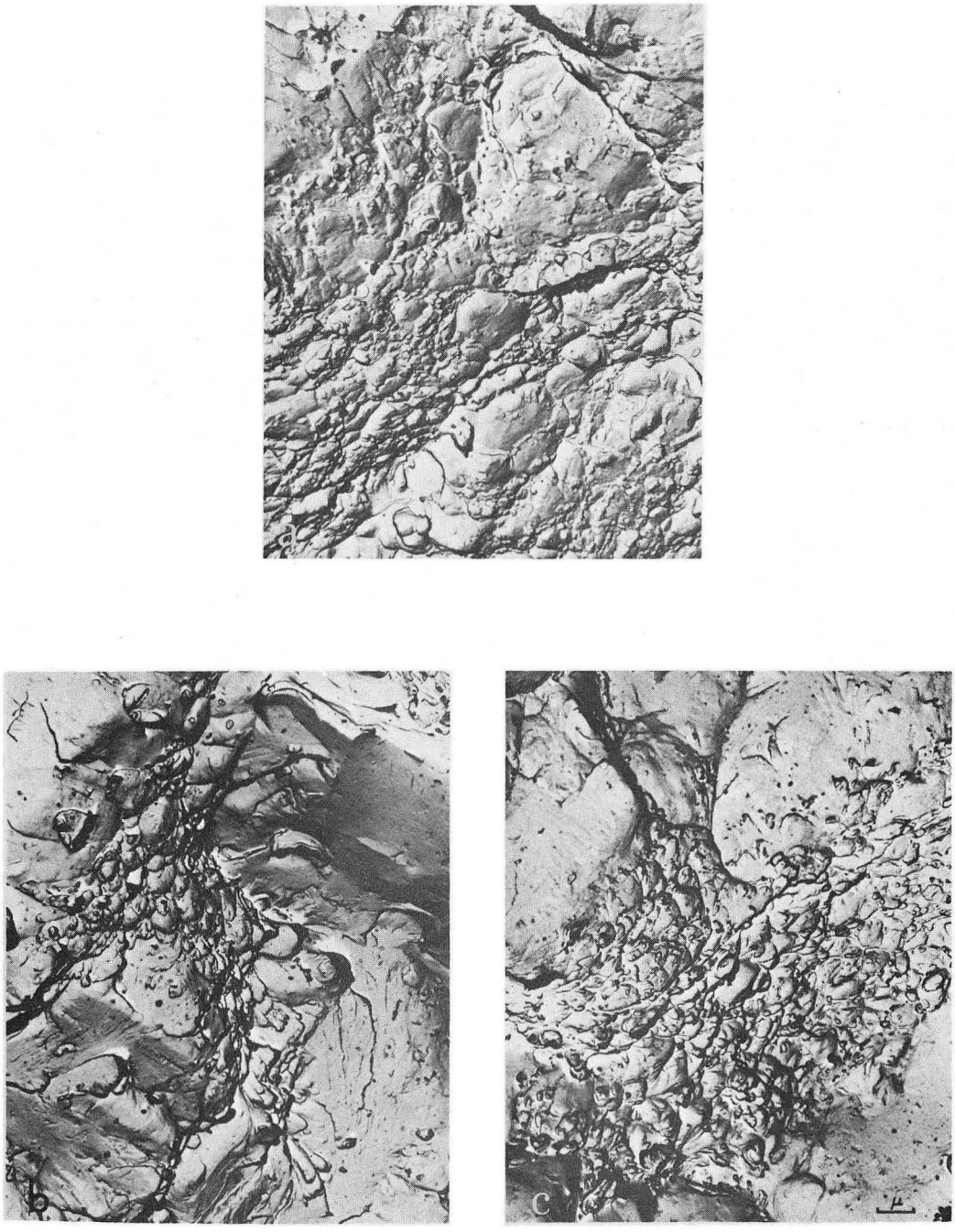

XBB 698-5580-A

Fig. 38

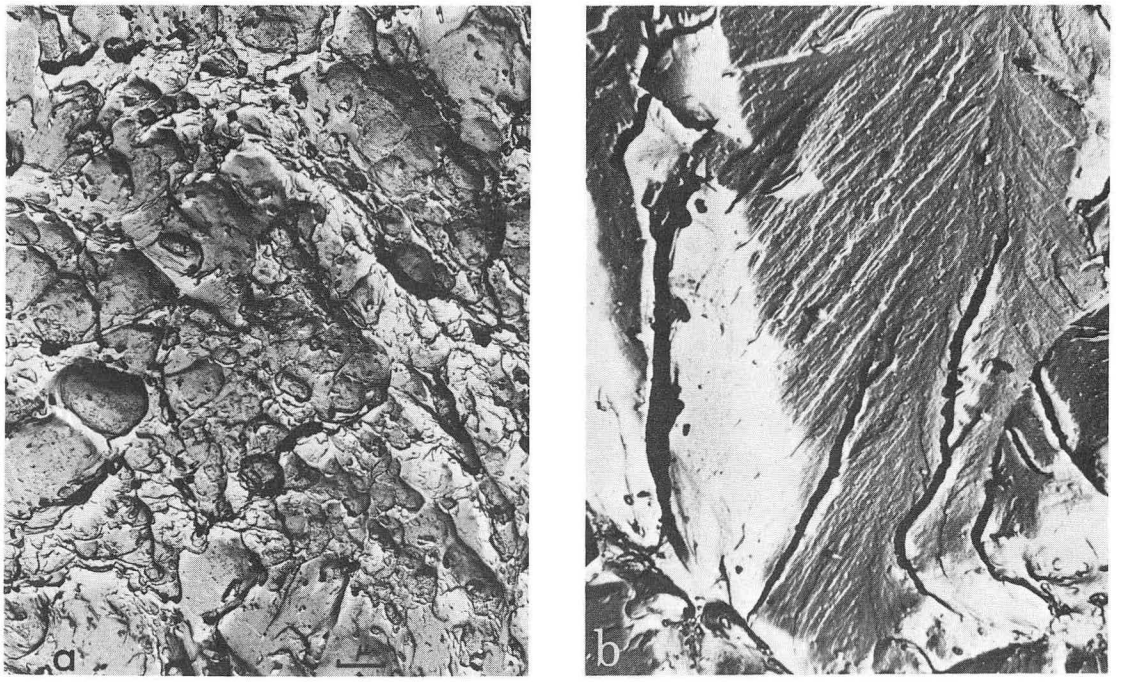

XBB 698-5559-A

Fig. 39

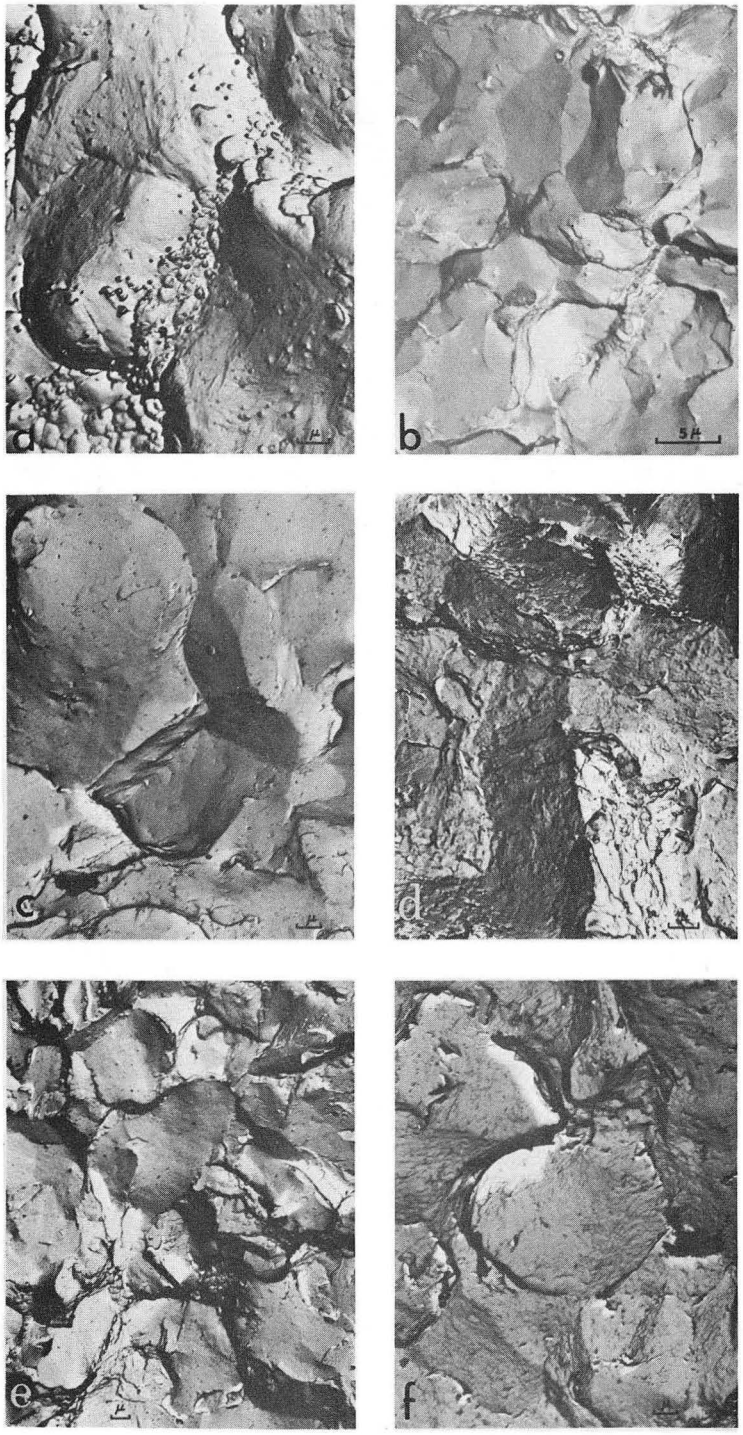

XBB 698-5585-A

Fig. 40

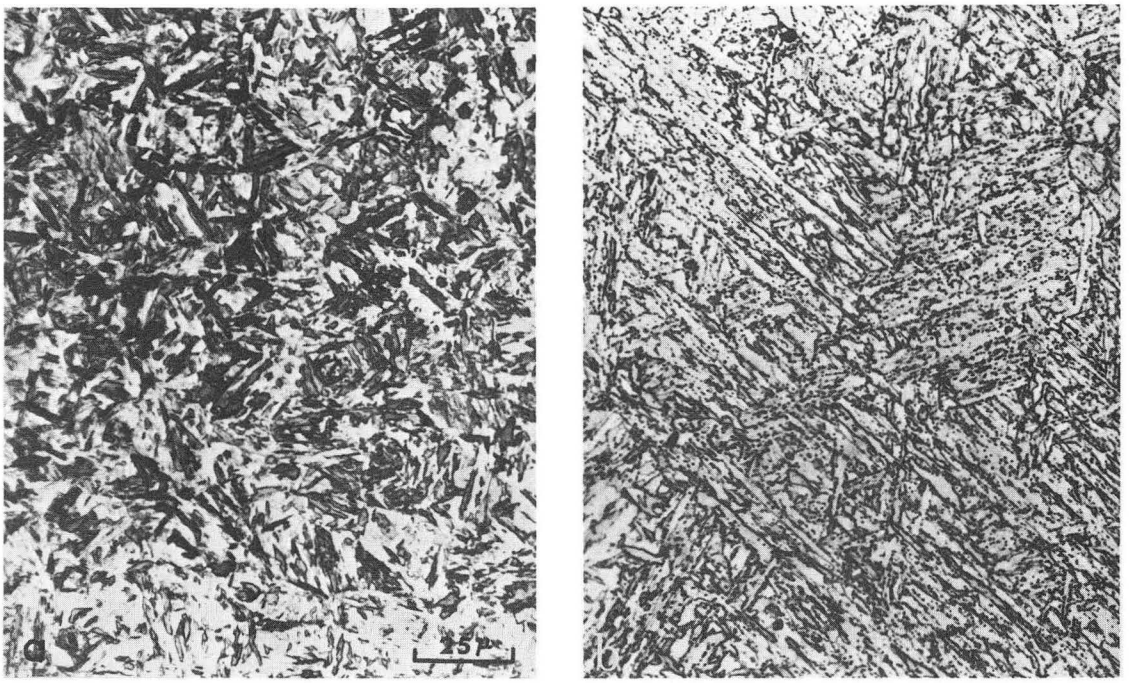

XBB 698-5570-A

Fig. 41

XBB 698-5565

Fig. 42

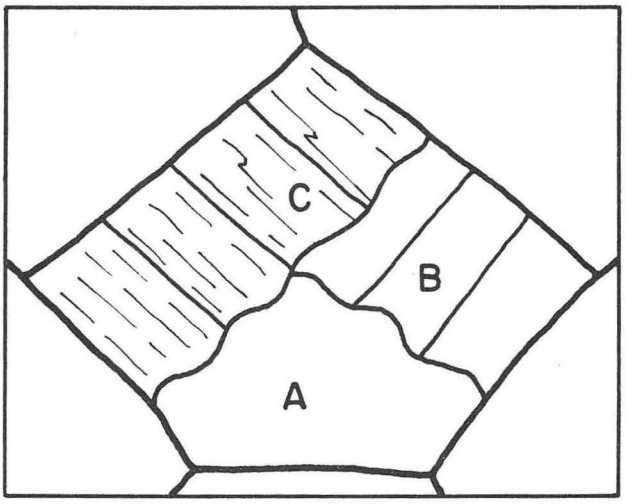

XBL 698-1315

Fig. 43

LEGAL NOTICE

This report was prepared as an account of Government sponsored work. Neither the United States, nor the Commission, nor any person acting on behalf of the Commission:

A. Makes any warranty or representation, expressed or implied, with respect to the accuracy, completeness, or usefulness of the information contained in this report, or that the use of any information, apparatus, method, or process disclosed in this report may not infringe privately owned rights; or

B. Assumes any liabilities with respect to the use of, or for damages resulting from the use of any information, apparatus, method, or process disclosed in this report.

As used in the above, "person acting on behalf of the Commission" includes any employee or contractor of the Commission, or employee of such contractor, to the extent that such employee or contractor of the Commission, or employee of such contractor prepares, disseminates, or provides access to, any information pursuant to his employment or contract with the Commission, or his employment with such contractor.

TECHNICAL INFORMATION DIVISION
LAWRENCE RADIATION LABORATORY
UNIVERSITY OF CALIFORNIA
BERKELEY, CALIFORNIA 94720